micro

Review

Nanocurcumin and Curcumin-Loaded Nanoparticles in Antimicrobial Photodynamic Therapy: Mechanisms and Emerging Applications

Edith Dube * and Grace Emily Okuthe

Department of Biological & Environmental Sciences, Walter Sisulu University, Mthatha 5117, South Africa; gokuthe@wsu.ac.za
* Correspondence: edube@wsu.ac.za

Abstract

The growing threat of antimicrobial resistance has necessitated the development of alternative, non-antibiotic therapies for effective microbial control. Antimicrobial photodynamic therapy, which uses photosensitizers activated by light to generate reactive oxygen species, offers a promising solution. Among natural photosensitizers, curcumin, a polyphenolic compound from *Curcuma longa*, has demonstrated broad-spectrum antimicrobial activity through reactive oxygen species-mediated membrane disruption and intracellular damage. However, curcumin's poor water solubility, low stability, and limited bioavailability hinder its clinical utility. Nanotechnology has emerged as a transformative strategy to overcome these limitations. This review comprehensively explores advances in nanocurcumin- and curcumin-loaded nanoparticles, highlighting their physicochemical enhancements, photodynamic mechanisms, and antimicrobial efficacy against multidrug-resistant and biofilm-associated pathogens. A range of nanocarriers, including chitosan, liposomes, nanobubbles, hybrid metal composites, metal–organic frameworks, and covalent organic frameworks, demonstrate improved microbial targeting, light activation efficiency, and therapeutic outcomes. Applications span wound healing, dental disinfection, food preservation, water treatment, and medical device sterilization. Conclusions and future directions are given, emphasizing the integration of smart nanocarriers and combinatorial therapies to enhance curcumin's clinical translation.

Keywords: nanocurcumin; photodynamic therapy; reactive oxygen species; antimicrobial; pathogen

check for updates

Academic Editors: Vasco D. B. Bonifácio and Sandra Pinto

Received: 21 July 2025
Revised: 7 August 2025
Accepted: 15 August 2025
Published: 18 August 2025

Citation: Dube, E.; Okuthe, G.E. Nanocurcumin and Curcumin-Loaded Nanoparticles in Antimicrobial Photodynamic Therapy: Mechanisms and Emerging Applications. *Micro* **2025**, *5*, 39. https://doi.org/10.3390/micro5030039

1. Introduction

Antimicrobial resistance (AMR) is a growing global health crisis that threatens the effective treatment of infectious diseases, leading to prolonged illness, increased mortality, and rising healthcare costs. The overuse and misuse of conventional antibiotics have accelerated the emergence of multidrug-resistant (MDR) pathogens [1,2], prompting an urgent need for alternative, non-antibiotic strategies to manage microbial infections. Among emerging technologies, antimicrobial photodynamic therapy (aPDT) has gained attention as a promising approach to overcome AMR by utilizing light-activated photosensitizers (PSs) to produce reactive oxygen species (ROS) that selectively destroy microbial cells [3] as illustrated in Figure 1, without contributing to resistance development.

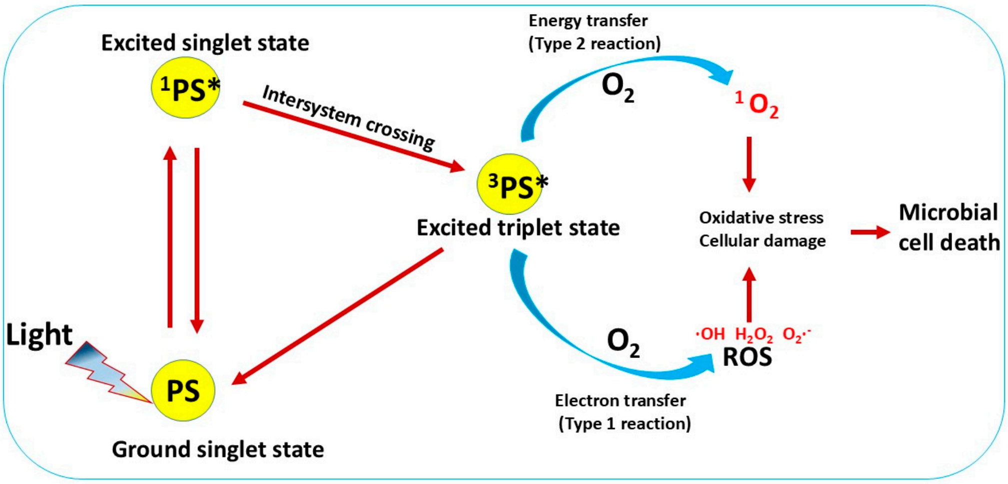

Figure 1. Illustration of aPDT through type 1 and type 2 reactions resulting in microbial cell death.

Natural product-based PSs play a pivotal role in aPDT due to their safety, biocompatibility, and ability to generate ROS upon light activation. When exposed to light of a specific wavelength, these PSs transition from their ground singlet state to an excited singlet state [4], as illustrated in Figure 1. If the excited PS does not return to the ground state, it undergoes intersystem crossing to form a triplet excited state, which is central to ROS production.

From the triplet state, two primary photochemical pathways can occur: Type I and Type II reactions. In a Type I reaction, the excited PS transfers a hydrogen atom or electron to surrounding biomolecules, forming radicals. These radicals then react with molecular oxygen through redox processes to produce superoxide anion radicals ($O_2\bullet^-$) and other ROS. In contrast, a Type II reaction involves the direct transfer of energy from the excited PS to molecular oxygen, generating singlet oxygen ($^1O_2$), a highly reactive and cytotoxic species [5]. The Type II mechanism is generally simpler and often more dominant in biological systems.

aPDT leverages these mechanisms to induce oxidative damage in microbial cells. The generated ROS attacks cellular components such as lipids, proteins, and nucleic acids, leading to membrane disruption, metabolic interference, and ultimately cell death [6]. This approach is effective against a wide range of pathogens, including bacteria, fungi, and viruses, even those in biofilm states or resistant to antibiotics. Moreover, aPDT offers significant advantages such as localized action, minimal toxicity to host tissues, and no risk of resistance development with repeated use [7]. The use of natural PSs, particularly curcumin, further enhances aPDT's appeal due to their safety, biodegradability, and environmental compatibility, offering an attractive alternative to synthetic dyes.

Curcumin, a polyphenolic compound extracted from the rhizome of *Curcuma longa*, has attracted significant interest due to its broad-spectrum antimicrobial, anti-inflammatory, antioxidant, and anticancer properties [8]. Curcumin naturally acts as a PS, producing ROS under blue light irradiation, and has demonstrated notable efficacy in the photodynamic inactivation of both planktonic and biofilm-associated pathogens [9]. However, its clinical translation remains limited by several drawbacks, including poor water solubility, low chemical stability, rapid photodegradation, low systemic bioavailability, and limited membrane permeability, which collectively impair its therapeutic performance in biological systems [10].

To overcome these limitations, the use of nanocurcumin (nCur) [11,12] and development of nanoparticle-based curcumin delivery systems [13,14] has emerged as a transformative solution. Encapsulation of curcumin into nanoscale carriers, such as liposomes, solid lipid nanoparticles (NPs), polymeric NPs, nanobubbles, metal-based nanocomposites, metal–organic frameworks (MOFs) and covalent organic frameworks (COFs), greatly enhances its solubility, stability, and bioavailability [15]. These nanocarriers also improve microbial targeting, promote controlled release, protect curcumin from premature degradation, and boost intracellular ROS generation, thereby enhancing photodynamic efficacy. This has led to the emergence of a new class of advanced therapeutic agents: nCur and curcumin-loaded NPs, which are particularly effective against MDR and biofilm-forming pathogens [16].

This review provides a comprehensive overview of recent advances in the design and application of nCur-based systems in aPDT. It discusses their mechanisms of action, highlights their advantages over free curcumin, and explores their potential for addressing critical challenges in modern infectious disease management. Figure 2 illustrates the steady increase in scientific publications related to the application of nanocurcumin- and curcumin-loaded nanoparticles in aPDT from 2011 to 2025.

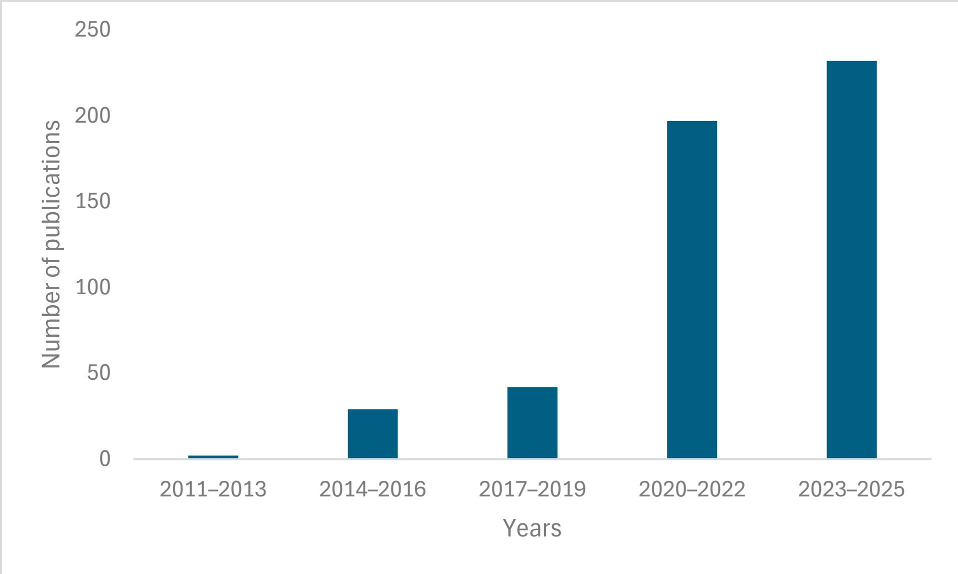

Figure 2. Trends in publications on nanocurcumin- and curcumin-loaded nanoparticles for aPDT (2011–2025).

The data shows a significant surge in research activity beginning in 2020, indicating heightened scientific interest and recognition of these nanostructured formulations as effective antimicrobial agents. This upward trend highlight the expanding role of nanotechnology in antimicrobial interventions and highlights the promising potential of curcumin as a PS in addressing the global challenge of antimicrobial resistance.

2. Curcumin as a Natural Photosensitizer

Antimicrobial curcumin has gained considerable attention as a PS in aPDT due to its favorable photophysical properties and broad-spectrum antimicrobial activity [17,18]. Its chemical structure, featuring conjugated double bonds and phenolic hydroxyl groups, allows it to absorb visible light, particularly in the blue region around 420–450 nm, and transition to an excited state capable of generating ROS [17]. As illustrated in Figure 3, upon light activation, curcumin undergoes intersystem crossing to produce $^1O_2$ and other ROS, which in turn induce oxidative damage to microbial membranes, proteins, and nucleic acids, leading to cell death. This mechanism supports the use of curcumin-based aPDT in areas such as wound healing, dental care, food preservation, and surface disinfection, among others.

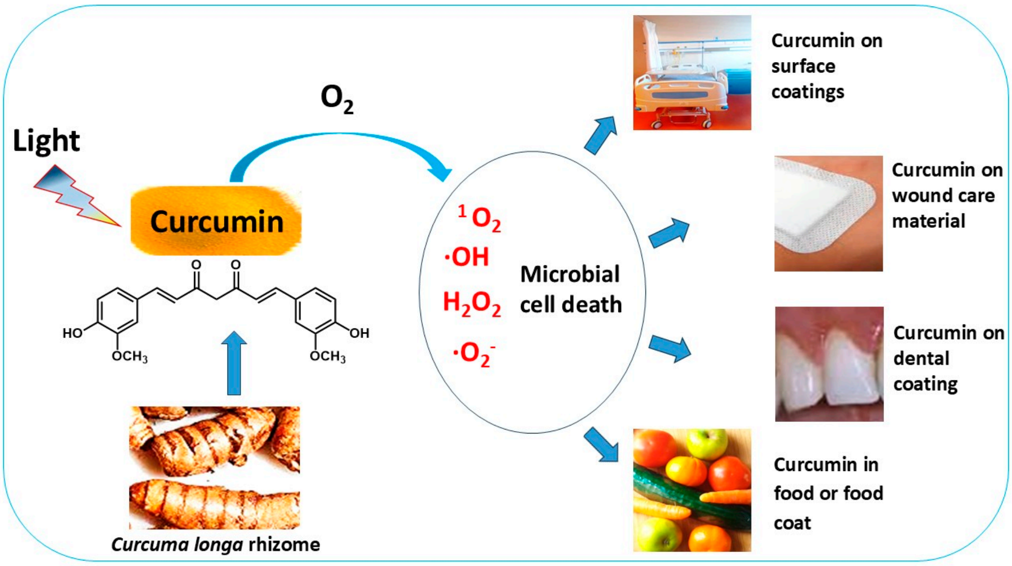

Figure 3. Illustration of curcumin-based aPDT and its potential applications, including wound healing, dental therapies, food preservation, and surface disinfection.

Several studies have reported the aPDT of curcumin. For example, Dang et al. (2025) reported complete inactivation of *Mycobacterium abscessus* using aPDT with 100 µM curcumin and a light dose of 48 J/cm^2. This treatment led to a 5.32-fold increase in intracellular ROS compared to untreated controls, highlighting oxidative stress as the key driver of curcumin's phototoxicity. The accumulated ROS caused oxidative damage to critical cellular components, including lipids, proteins, and nucleic acids, ultimately resulting in cell death. Significant membrane disruption was also observed, evidenced by a 9.53-fold increase in fluorescence intensity, indicating compromised membrane integrity that likely enhanced ROS penetration and intensified intracellular damage. Transmission electron microscopy (TEM) confirmed extensive structural breakdown, including cell wall degradation, membrane rupture, and cytoplasmic disintegration [19]. These results demonstrate the multifaceted antimicrobial action of curcumin-based aPDT, targeting both external and internal bacterial structures to ensure total inactivation. Similarly, Yuan et al. (2022) found that aPDT inflicted multiple forms of damage on *Staphylococcus aureus*. Morphological effects included membrane collapse, leakage of intracellular contents, and increased cell aggregation, with severity escalating alongside light dose. Membrane permeability was significantly altered, as shown by increased absorbance at OD260 and OD280, indicating the release of DNA and proteins. Flow cytometry with double staining revealed progressive loss of membrane integrity and esterase activity, with the proportion of damaged cells increasing with light exposure. Sublethal cell populations initially rose and then declined, suggesting a transition from reversible injury to irreversible cell death. Intracellular ROS levels also rose markedly following aPDT, disrupting membrane function and inducing cell death, an effect significantly reduced by ROS scavengers, further confirming the central role of ROS in the antimicrobial mechanism [20]. Table 1 summarizes various studies that demonstrate the antimicrobial efficacy of curcumin-based aPDT under different experimental conditions, highlighting the influence of formulation type, curcumin concentration, light parameters, and treatment environment on overall effectiveness.

Table 1. Summary of curcumin-based aPDT against different bacteria and light settings.

Curcumin Concentration	Light Dosage	Effect	Ref
CuminUP60® vs. natural curcumin, 10.42–333.3 µM	light-emitting diode (LED, 425 ± 20 nm), 5.3 mW/cm^2 for 30 min (9.54 J/cm^2)	Both curcumin forms exhibited broad-spectrum bactericidal activity against multiple bacteria including *S. aureus*, *Listeria monocytogenes*, *Escherichia coli*, *Vibrio parahaemolyticus*, *Shewanella putrefaciens*, and *Pseudomonas fluorescens*.	[9]
5 g/L and 3 g/L	LED (450 nm), 1200 mW/cm^2, irradiance 738 mW/cm^2	At 3 g/L, curcumin reduced *Lactobacillus casei* by 99.5%, comparable to chlorhexidine (100%) and exceeding non-irradiated curcumin (60.3%).	[21]
60 µg/mL (*S. aureus*), 100 µg/mL (*E. coli*)	Laser (405 nm), 14 mW/cm^2, 40 min	Curcumin achieved 93.2% antibacterial rate against *S. aureus* and 42.6% against *E. coli*.	[22]
5 mg/mL	LED (390–480 nm), 1000 ± 100 mW/cm^2, 60 s (60 J/cm^2)	*E. faecalis* count reduced by 1.35 $\log_{10}$ CFU/mL; more effective than curcumin alone(1.73 $\log_{10}$ CFU/mL), untreated control (3.03 $\log_{10}$ CFU/mL), and LED alone (2.90 $\log_{10}$ CFU/mL).	[23]
0.25% and 10.0% Curcumin-loaded varnish	LED (440–460 nm), 19 mW/cm^2 for 15–60 min (17.4–69.7 J/cm^2)	Increased curcumin loading and light dose enhanced photoelimination of *S. mutans* and *Candida albicans*.	[24]
100 µM	50 W xenon lamp (400–780 nm), 48 J/cm^2	Complete inactivation of *M. abscessus*.	[19]
10 µM	LED (440 ± 5 nm), 3.6 × 10^{-3} W/cm^2, 1.296–2.592 J/cm^2	aPDT reduced *S. aureus* by 6.9 log CFU/mL in phosphate-buffered saline (PBS). Efficacy declined in fruit juices due to ROS quenching; pineapple was more responsive than mango; carrot juice showed no effect. At 2.592 J/cm^2, no *S. aureus* was detectable in mango/pineapple juice.	[20]
0.05%	LED (480 nm), 72 J/cm^2	In root canal treatment, curcumin-aPDT achieved 34% reduction in *E. coli* CFU, with 12% standard deviation.	[25]
1–5 µM	Diode laser (445 nm), 0.25 W/cm^2, 15 J/cm^2	Curcumin combined with blue light irradiation reduced SARS-CoV-2 viral load by >99% in vitro, despite the concentrations alone showing no antiviral activity	[26]

As shown in Table 1, across multiple studies, curcumin consistently exhibited broad-spectrum antimicrobial activity, with optimal outcomes achieved at higher concentrations (≥100 µM or >3 g/L) and light fluences above 9 J/cm^2. Significant reductions in bacterial viability were reported against key pathogens such as *S. aureus*, *E. coli*, *L. casei*, and *M. abscessus* [9,19,21]. The effectiveness of curcumin was further enhanced by advanced formulations such as CuminUP60® and curcumin-loaded varnishes [9,24]. However, treatment matrices substantially influenced outcomes; while clear media like PBS allowed for high efficacy, complex environments such as fruit juices and root canals, due to turbidity, pigment absorption, and ROS quenchers, diminished photodynamic performance [20]. Despite these challenges, curcumin-based aPDT demonstrated comparable antimicrobial efficacy to conventional agents like chlorhexidine in some cases, supporting its potential as a versatile, natural alternative for pathogen control across clinical and food-related settings.

Curcumin exhibits antimicrobial activity against a wide range of pathogens, including Gram-positive and Gram-negative bacteria, fungi such as *C. albicans*, and even some viruses [18,27]. This broad-spectrum efficacy, combined with its low toxicity to mammalian cells under controlled doses, makes curcumin an attractive alternative to synthetic PSs in aPDT applications for wound care, dental treatment, food preservation, and surface disinfection. However, the clinical translation of curcumin in aPDT is hindered by several challenges.

The main challenges include its extremely low aqueous solubility (<0.0006 mg/mL) [28], poor chemical stability at physiological pH, rapid metabolic degradation, and limited bioavailability, all of which significantly limit its bioavailability and therapeutic efficacy [29]. While its solubility is markedly improved in organic solvents such as ethanol (~1–5.6 mg/mL) [30,31], acetone (~7.75 mg/mL) [31], DMSO (~20 mg/mL) [30,31], and PEG-400 (up to 250 mg/mL) [32], these are not ideal for biological use. Additionally, curcumin is highly photosensitive and undergoes rapid degradation under UV and blue light due to photooxidation and bond cleavage, leading to reduced therapeutic efficacy. For instance, it exhibits a 42.1% degradation rate after 10 min of blue light exposure, about 1.7 times higher than under red light [33]. This accelerated photobleaching results from strong absorption in the blue region, which enhances photoexcitation and ROS generation. These findings highlight the importance of optimizing light wavelength and formulation strategies to balance activation efficiency with molecular stability. Furthermore, chemical stability is influenced by environmental conditions such as pH, solvent polarity, and oxygen levels. For instance, in basic solutions (pH > 7.0), the half-life of curcumin is around 10 min, whereas at pH = 3.0–6.5, the half-life of curcumin is approximately 200 min [34]. In terms of photodynamic efficiency, curcumin's singlet oxygen quantum yield is solvent-dependent, ranging from 0.04 in ethanol [35] to 0.372 in THF [36], but is significantly lower in aqueous systems due to aggregation and quenching effects [17]. Despite these challenges limiting the clinical application of free curcumin as a PS, it possesses several notable advantages over synthetic alternatives such as methylene blue and porphyrins, including its natural origin, low toxicity to mammalian cells, and high biocompatibility. These attributes have driven efforts to enhance its bioavailability and therapeutic efficacy, leading to extensive exploration of nanotechnology-based approaches. Encapsulation of curcumin into various nanocarriers, such as liposomes, polymeric NPs, micelles, dendrimers, solid lipid NPs, and nanostructured lipid carriers, has been shown to improve its aqueous solubility, protect against enzymatic and photodegradation, and enhance cellular uptake and photoactivation under light exposure [37,38]. These nanoformulations not only enhance curcumin's singlet oxygen generation but also allow for better control over light-mediated cytotoxic effects. Together, these advancements significantly expand the potential of curcumin as an efficient and biocompatible PS in aPDT.

3. Nanocurcumin (nCur), Curcumin Encapsulated or Conjugated Within Nanocarriers for aPDT

As discussed in the previous section, the clinical application of free curcumin in aPDT is significantly hindered by its poor water solubility, low chemical stability, rapid degradation, and limited bioavailability. To address these challenges, considerable research has focused on nanotechnology-based strategies that improve the pharmacokinetic and photodynamic properties of curcumin. Among these, nCur, a nanosized formulation of curcumin, and various curcumin-loaded nanocarriers have shown substantial promise [11,39]. These nanoplatforms enhance solubility, protect against degradation, and facilitate efficient intracellular delivery [40], thereby amplifying ROS production under light activation. This section explores recent advances in the development and application of nCur (Section 3.1) and curcumin-loaded nanocarriers (Section 3.2) for improved aPDT performance, with a particular focus on their antimicrobial efficacy, formulation-dependent effects, and potential for overcoming drug-resistant infections and biofilms.

3.1. Nanocurcumin (nCur) for Enhanced aPDT

The development of nCur has significantly advanced the use of curcumin in aPDT by overcoming the major limitations of its free form [38]. Numerous in vitro studies have demonstrated that nCur exhibits broad-spectrum antimicrobial activity, effectively targeting Gram-positive bacteria (e.g., *S. aureus*, *Enterococcus faecalis*), Gram-negative bacteria (e.g., *E. coli*, *Pseudomonas aeruginosa*), and fungi (*C. albicans*), as well as biofilm-forming and MDR strains [16,41]. The improved photodynamic response of nCur across these studies reflects its enhanced physicochemical properties and its ability to penetrate complex microbial structures such as biofilms [11]. Table 2 shows the aPDT effect of nCur against different microbes.

Table 2. Antimicrobial efficacy of nCur-based PDT under varying concentrations, light sources, and formulations.

nCur Size	nCur Concentration	Light Dosage	Effect	Ref
-	3 g/L	Blue LED emitting at 385–515 nm, output intensity of 1200 mW/cm^2, irradiance, 738 mW/cm^2	aPDT significantly reduced *Streptococcus mutans* viability, with curcumin (3 g/L) achieving a 99.7% reduction, while nano-curcumin showed lower effectiveness, reaching 82.3% reduction	[42]
9.5 ± 0.1 nm	0.5% nCur in 0.9% sodium chloride solution	LED with wavelength of 450 nm, power density was 1 W/cm^2, energy density was 60 J/cm^2 and irradiation duration was 60 s	aPDT) achieved the greatest reduction in dual-species *S. mutans* and *Lactobacillus acidophilus* biofilms, with 40% reduction compared to nCur alone (24.53%).	[11]
100 nm	-	Laser (980 nm), Power: 0.5 W, irradiation duration was 20 s	Laser-activated nCur demonstrated significant antimicrobial effects against both *E. faecalis* and *C. albicans*	[12]
-	nCur was added to Activa BioActive Base/Liner (ABBL) in 0.5%, 1%, 2%, and 5% (*w*/*w*) concentrations to fabricate nCur-ABBL disks	LED (435 ± 20 nm), output intensity 1000–1400 mW/cm^2, dose 300–420 J/cm^2, duration 5 min	After 60 days of aging, 5% nCur-ABBL disks activated by aPDT showed a 97.75% reduction in *S. mutans* colonies, while 2% nCur-ABBL discs showed a 96.25% reduction	[43]
-	3 g/L	LED (450 nm), power intensity of 1200 mW/cm^2, irradiance 738 mW/cm^2	aPDT using nCur achieved a 96.5% reduction in *L. casei* biofilms, closely approaching the complete inhibition observed with the positive control, chlorhexidine digluconate (CHX, 100%).	[21]

Table 2. *Cont.*

nCur Size	nCur Concentration	Light Dosage	Effect	Ref
-	5 mg/mL	LED (390 to 480 nm), power density of 1000 ± 100 mW/cm^2, irradiation time of 60 s, energy density was 60 J/cm^2	nCur-mediated aPDT significantly reduced *E. faecalis* count (1.22 $\log_{10}$ CFU/mL) versus curcumin alone (1.71), untreated control (3.03), and LED alone (2.90).	[23]
-	3.1 mM. 6.2 mM and 12.5 mM	28.7 mW/cm^2 + 2 min laser, 45.2 mW/cm^2 + 3 min laser and 45.2 mW/cm^2 + 4 min laser	Significant reduction in Acinetobacter *baumannii* viability and modulating its virulence gene expression.	[44]

Table 2 summarizes the antimicrobial effects of nCur-based aPDT under different concentrations, formulations, and light settings against pathogens such as *S. mutans*, *L. acidophilus*, *L. casei*, *E. faecalis*, *C. albicans*, and *A. baumannii*. Overall, nCur-mediated aPDT demonstrated consistent and significant antimicrobial activity across a range of experimental setups. For example, nCur at 3 g/L reduced *L. casei* biofilms by 96.5% under high-intensity LED (450 nm), closely approximating the efficacy of the positive control, chlorhexidine (100%) [21]. In dual-species biofilms of *S. mutans* and *L. acidophilus*, light-activated nCur reduced bacterial load by 40%, compared to 24.5% for nCur alone, showing the added benefit of photodynamic activation [11].

However, not all nanoformulations perform equally. In one study, nCur (3 g/L) demonstrated significantly lower antibacterial efficacy against *S. mutans* compared to free curcumin. Under light exposure, nCur achieved 82.3% and 54.9% reductions in planktonic and biofilm forms, respectively, whereas free curcumin reached 99.7% and 76.5% [42]. This reduced efficacy may result from the nanomicellar formulation, which, while improving solubility, may increase viscosity or adhesiveness, hindering diffusion into the biofilm matrix. Nanoparticle aggregation further limits performance due to van der Waals and hydrophobic interactions, poor surface charge (zeta potential $< \pm 20$ mV), or inadequate steric stabilization [45]. These conditions reduce NP dispersion, light absorption, and ROS generation. Additionally, biofilms act as physical and chemical barriers through size-exclusion effects, electrostatic trapping by negatively charged extracellular polymeric substances, high matrix viscosity, and chemical sequestration or inactivation of curcumin [46]. Hypoxic zones in deeper layers further restrict ROS generation. These combined challenges reduce curcumin availability, impair uniform activation, and compromise aPDT outcomes. To overcome these barriers, NP designs should incorporate strategies such as PEGylation, size optimization (<100 nm), surface charge modulation, enzymatic matrix disruption, and stimuli-responsive release systems to enhance biofilm penetration, improve curcumin activation, and maximize therapeutic efficacy [47].

By contrast, a separate study incorporating nCur into Activa BioActive Base/Liner (ABBL) as composite disks (0.5–5% *w*/*w*) showed superior and long-lasting efficacy. After LED irradiation (300–420 J/cm^2 for 5 min), 5% nCur-ABBL disks achieved a 97.75% reduction in *S. mutans* viability after 60 days, compared to 96.25% for 2% disks. Increased nCur concentration and aging time produced a synergistic effect; for example, raising the concentration from 1% to 2% led to an increase in biofilm reduction from 79.1% at 30 days to 88% at 60 days [43]. This enhanced efficacy was likely due to the ABBL matrix's ability to improve curcumin retention, stability, and sustained release, as well as better contact with the biofilm surface and more efficient ROS generation.

Furthermore, nCur-based aPDT proved effective against resistant organisms like *E. faecalis*, *C. albicans*, and *A. baumannii*. In *A. baumannii*, it also modulated virulence gene expression. Studies employing combined light sources (e.g., laser + LED) and varied light fluences demonstrated enhanced antimicrobial outcomes, confirming that both the delivery system and light parameters play critical roles in aPDT efficacy.

While nCur enhances curcumin's solubility and bioavailability, its therapeutic impact depends significantly on formulation type, target pathogen, and light conditions. Solid-state systems such as ABBL composites offer promising solutions for overcoming biofilm penetration and ensuring sustained antimicrobial activity, reinforcing the potential of nanocurcumin-based aPDT for various applications.

3.2. Curcumin Nanoconjugate and Nanocarriers for Enhanced aPDT

The incorporation of curcumin into NP-based delivery systems has proven to be a transformative strategy in overcoming the physicochemical and biological limitations that hinder its clinical application in aPDT [48]. While curcumin is well-known for its inherent antimicrobial and photodynamic properties, its direct application is restricted by poor water solubility, low systemic bioavailability, rapid photodegradation, and weak interaction with bacterial membranes due to its negative surface charge [49]. Nanocarriers offer a robust solution by enhancing curcumin's solubility, protecting it from degradation, enabling targeted or stimulus-responsive release, improving cellular uptake, and amplifying ROS generation upon light activation, all critical factors for effective aPDT [48,50,51].

3.2.1. aPDT of Curcumin-Loaded Nanocarriers and Nanoconjugates

The formulations summarized in Table 3 showcase the diversity and efficacy of nanoplatforms used for curcumin delivery.

Table 3. Antimicrobial efficacy of curcumin nanoconjugates or nanocarriers-based PDT under varying concentrations, light sources, and formulations.

Curcumin Nanocarriers and Nanoconjugates	Curcumin Concentration	Light Dosage	Effect	Ref
Curcumin-loaded Chitosan (CT) NPs	0.04 and 0.08 mg/mL	Blue light at 450 nm, light intensity 28.84 mW/cm^2, irradiation time, 60 min	A reduction of more than 3 $\log_{10}$ CFU was observed in both *S. aureus* and *E. coli*	[13]
Curcumin loaded chitosan/sodium alginate NPs (Cur-CT-Alg NPs), 257.2 to 473.1 nm	-	LED (460 nm), Energy dose 15 J/cm^2 for 11 min and 53 s	Cur-CT-Alg NPs combined with aPDT significantly reduced *S. mutans* biofilms by 3 $\log_{10}$ CFU/mL	[52]
Curcumin-containing chitosan-shelled nanobubbles, (Cur-CT-NBs)	743 ± 44 µg/mL of NBs	LED, (425 nm to 470 nm) for 3 h	Cur-CT-NBs showed the following MIC values: for *E. coli*, 46.4 µg/mL with and without LED; for *S. aureus*, 92.8 µg/mL without LED and 46.4 µg/mL with LED; and for *E. faecalis*, 46.4 µg/mL without LED and 23.2 µg/mL with LED.	[39]

Table 3. *Cont.*

Curcumin Nanocarriers and Nanoconjugates	Curcumin Concentration	Light Dosage	Effect	Ref
Oxygen-loaded curcumin-containing nanobubbles, (Cur-Oxy-CT-NBs)	743 ± 49 μg/mL of NBs	LED (425 nm to 470 nm) for 3 h	Cur-Oxy-CT-NBs exhibited enhanced antibacterial activity, with minimum inhibitory concentrations (MICs) as follows: for *E. coli*, 92.8 μg/mL without LED and 46.4 μg/mL with LED; for *S. aureus*, 46.4 μg/mL without LED and 11.6 μg/mL with LED; and for *E. faecalis*, 92.8 μg/mL without LED and 46.4 μg/mL with LED.	[39]
Curcumin-loaded solid lipid NPs (SLNPs-composed of cetyl palmitate and Tween® 80) within an alginate-based hydrogel matrix	20% (*v*/*v*), and 50% (*v*/*v*) Cur-SLN in hydrogel	LED (430–490 nm) for 150 s	Photoactivated formulations reduced *E. faecalis* biofilms by 70%, outperforming non-photoactivated (45%)	[14]
Indocyanine green (ICG) doped with nano-curcumin and conjugated with Metformin (Met) (Cur-ICG-Met NPs), 60–100 nm	Cur-ICG-Met NPs consist of 100 mg of Cur NPs, 1000 μg/mL of ICG, and 10 mM of Met and 10 μL of Cur-ICG-Met NPs was used for aPDT	Diode Laser (810 nm), Energy density: 31.2 J/cm^2 and power output capacity: 200 mW and LED (450 nm), Energy density: 60 J/cm^2 and power output intensity: 500 mW/cm^2	The dual-wavelength irradiation technique (diode laser + LED) effectively reduced viable *E. faecalis* within biofilm structures, achieving a cell viability reduction ranging from 82.74% to 83.84%.	[53]
nCur-AgNPs-colistin (CL) (402.6 nm)	250 μg/mL	LED light (450 ± 10 nm), Output Power: 200 mW, Power Density: 0.51 W/cm^2, Exposure Time: 14 min (energy density was 476 J/cm^2).	Reduced the formation of biofilm in *P. aeruginosa*	[50]
Lysozyme (Lys)-gold nanocluster (AuNCs)-Cur conjugate, (Lys-AuNCs-Cur) (Lys-AuNCs = 5 nm)	10 to 60 μg/mL for *S. aureus* Up to 100 μg/mL for *E. coli* Up to 100 μg/mL for MRSA	Laser light (405 nm), intensity was 14 mW/cm^2, exposure time 40 min	Lys-AuNCs-Cur exhibited greater antibacterial activity against *S. aureus* and *E. coli* than free curcumin and effectively eradicated MRSA.	[22]

Table 3. *Cont.*

Curcumin Nanocarriers and Nanoconjugates	Curcumin Concentration	Light Dosage	Effect	Ref
Cur-silica NPs (36 to 40 nm)	1 mg/mL	LED (465 nm), power density was 34 mW/cm^2, irradiation time was 10 min, light dose was 20 J/cm^2	Cur–silica NPs caused a significant reduction of more than 6 $\log_{10}$ CFU in the growth of both *S. aureus* and *P. aeruginosa* planktonic cells.	[51]
Curcumin encapsulated in poly (lactic-co-glycolic acid) (PLGA) NPs (Cur@PLGA-NPs)	10% weight (wt.)	Blue laser (450 ± 10 nm), output intensity of 1.6 W/cm^2, 522.8 J/cm^2,	Cur@PLGA-NPs demonstrated in vitro anti-COVID-19 activity by significantly reducing SARS-CoV-2 titers in infected plasma.	[54]
Curcumin encapsulated into zeolite imidazole framework-8 (ZIF-8) NPs, and coated with ethylated poly-L-lysine (PLL) and loaded with ciprofloxacin (CIP) (Cur@ZIF-8 NPs/PLL-CIP, 325.9 nm)	In vitro, the Cur concentration was 16 µg/mL at a Cur@ZIF-8 NPs/PLL-CIP dose of 500 µg/mL, while in vivo wound healing studies in mice used 8 µg/mL Cur at a NP dose of 250 µg/mL.	Blue light (430 nm), intensity of 10 mW/cm^2 for 10 min in vitro and 20 min in vivo	Cur@ZIF-8 NPs/PLL-CIP enable ROS-responsive drug release and curcumin-triggered photodynamic therapy, effectively killing methicillin-resistant *S. aureus* (MRSA) (98.06%) and disrupting biofilms (99.83%) under 430 nm light with H_2O_2. In MRSA-infected mice, they accelerated wound healing (98.81% rate in 11 days) and restored normal skin structure, demonstrating strong synergistic antimicrobial and therapeutic effects.	[55]
Curcumin/ polycaprolactone@zeolitic imidazolate framework-8 (Cur/PCL@ZIF-8, ~100–200 nm) composite film	Composite films contained ≥15% *w*/*w* Cur@ZIF-8	Blue light (420–430 nm), intensity of 2.2 mW/cm^2	Composite films loaded with more than 15% (*w*/*w*) Cur@ZIF-8 demonstrated a 99.9% reduction in *Escherichia coli* and *S. aureus*, alongside a strong anti-adhesion effect.	[56]
Cur@ZIF-8 NPs (150 nm, while ZIF-8 alone was 80 nm)	5 mg/mL	Blue light (420–430 nm), intensity of 2.2 mW/cm^2 for 1 h	Cur@ZIF-8 NPs exhibited strong antibacterial activity against *E. coli* and *S. aureus*, which was significantly enhanced under blue light. The combination triggered ROS overproduction and K^+ leakage, disrupting bacterial membranes. Cur@ZIF-8 NPs under light outperformed Cur alone,	[57]

Table 3. *Cont.*

Curcumin Nanocarriers and Nanoconjugates	Curcumin Concentration	Light Dosage	Effect	Ref
Curcumin and aggregation-induced emission luminogen (TTD), encapsulated into ZIF-8 (Cur-TTD@ZIF-8 NPs, 360.84 nm)	62.5 µg/mL (2MIC) against *S. aureus* and 125 µg/ mL (2MIC) against *P. aeruginosa*.	Blue light, 12 J/cm^2 (20 mW/cm^2 for 10 min)	Cur-TTD@ZIF-8 NPs provide bacteria targeting, fluorescence imaging, pH-responsive photodynamic therapy (PDT), and anti-inflammatory effects. Their positive charge enables targeting of *P. aeruginosa* and *S. aureus*, with red fluorescence aiding imaging. Under blue light, Cur release triggers ROS generation, yielding 99.94% and 99.84% antibacterial rates. In vivo, they reduced bacterial load, alleviated inflammation, and accelerated wound healing, promoting tissue regeneration, angiogenesis, collagen deposition	[58]
Oxygen- and curcumin-laden ionic liquid@silica nanocapsules (Cur-IL@SiNCs, 15–70 nm and 280–350 nm)	2 mg of Cur per gram of IL	Blue light LED Lamp, 5 W (450 nm)	Cur-IL@SiNCs in gelatin films showed a photodynamic antimicrobial effect under blue light, significantly reducing bacterial growth	[59]
Curcumin-based bioactive zinc-based metal–organic frameworks (Zn-MOF) and Ti_3C_2Tx MXene nanosheets (NSs) (Cur/Zn-MOF@Ti_3C_2Tx, lattice spacing of 0.22 nm)	12.5 to 200 µg/mL	Near-infrared (NIR) light (808 nm), 1.0 W/ cm^2 for 15 min	The Cur/Zn-MOF@Ti_3C_2Tx nanosheets combine photothermal therapy (49.7 °C, 38.2% efficiency), photodynamic ROS generation (•O_2^-, •OH, $^1O_2$), and NIR-triggered release of Zn^{2+} and curcumin. It kills *E. coli* and *S. aureus*, inhibits bacterial growth for 24 h, and accelerates infected wound healing (>99% closure in 8 days).	[60]

Table 3. *Cont.*

Curcumin Nanocarriers and Nanoconjugates	Curcumin Concentration	Light Dosage	Effect	Ref
Curcumin linked to tetrakis (4-carboxyphenyl) porphyrin TCPP (Cur-TCPP NPs) and co-coordinated with copper (Cu) and sodium alginate (SA) to form a covalent organic framework-like (COF-like) structure (800 nm long)	Cur-TCPP NPs were used at 10 mg/mL in hydrogel synthesis. For ROS detection, Cur-TCPP, and Cur-CuTCPP were tested at 0.5 mg/mL (as precursors: 112 mg TCPP, 72 mg Cur used).	Light (660 nm), 0.4 W/cm^2 for 20 min	The Cur -TCPP NPs COF hydrogel exhibited strong antibacterial activity, achieving 99.95% and 99.8% eradication of *S. aureus* and *E. coli*, respectively. It increased bacterial membrane permeability, causing protein leakage. In vivo, it reduced TNF-α, elevated IL-10 and VEGF expression, enhanced collagen deposition, and accelerated wound healing and cell migration.	[61]

Several nanoplatforms evaluated in Table 3 demonstrate aPDT enhancements across a broad spectrum of bacterial targets and SARS-CoV-2. Chitosan-based NPs, including Cur-CT and Cur-CT-Alg NPs, achieved >3 $\log_{10}$ CFU reductions in *S. aureus*, *E. coli*, and *S. mutans*, primarily due to the mucoadhesive and bioadhesive nature of chitosan, which promotes closer interaction with bacterial surfaces. Under blue LED light, these carriers significantly increased curcumin's bioavailability and antimicrobial effectiveness [13,52]. Polymeric NPs, particularly those made from biocompatible polymers such as CT and PLGA, have shown significant promise in enhancing curcumin delivery for aPDT [13,54]. These carriers offer several advantages, including protection of curcumin from photodegradation, sustained release profiles, and improved interaction with microbial cells.

Curcumin-loaded nanobubbles (Cur-CT-NBs and Cur-Oxy-CT-NBs) offered even greater performance, exhibiting species-dependent behavior. For instance, *S. aureus* and *E. faecalis* internalized the nanobubbles, enabling enhanced intracellular ROS generation and phototoxicity. Interestingly, even *E. coli*, which did not internalize the NBs, show membrane disruption and killing upon light exposure, indicating effective extracellular ROS activity. The oxygen-enriched nanobubbles amplified ROS generation, resulting in lower MIC values and longer-lasting antimicrobial effects against both Gram-positive and Gram-negative bacteria [39].

Other systems, such as solid lipid (SL) NPs embedded in alginate hydrogels, provided sustained curcumin release and better photostability. These features translated into higher biofilm reduction in E. *faecalis* under photoactivated conditions compared to dark controls [14]. Lipid-based NPs, including liposomes and SLNPs, significantly enhance the delivery and therapeutic performance of curcumin in aPDT. These carriers improve curcumin's solubility, protect it from degradation, and facilitate its transport across biological barriers. Their ability to encapsulate hydrophobic molecules enables deeper penetration into biofilms and infected tissues, where conventional treatments often fail [62]. Additionally, they offer sustained release and enhance ROS generation upon light activation, leading to improved antimicrobial efficacy against persistent and hard-to-treat infections.

Moreover, advanced multifunctional platforms such as Cur-ICG-Met NPs represent a promising strategy for enhancing aPDT. By integrating curcumin with indocyanine green and metformin, these nanocarriers exploit the complementary properties of each component. ICG enhances light absorption in the near-infrared (NIR) range, enabling deeper tissue penetration, while metformin modulates bacterial metabolism and enhances cellular stress responses. When activated with dual-wavelength irradiation, 810 nm (diode laser) and 450 nm (LED), this system significantly amplifies ROS production, leading to synergistic phototoxic effects. In vitro studies demonstrated that Cur-ICG-Met NPs achieved over 82% reduction in *E. faecalis* biofilm viability, highlighting their potential to overcome the protective barriers of biofilms and improve treatment outcomes in resistant infections [53]. This multifunctional approach shows the potential of combining photodynamic agents with metabolic modulators for more effective, targeted microbial eradication.

Hybrid formulations such as nCur-AgNPs-colistin [50] and Lys-AuNCs-Cur [22] demonstrated even more pronounced antimicrobial outcomes. The former effectively disrupted *P. aeruginosa* biofilms, while the latter eradicated *S. aureus*, *E. coli*, and MRSA with exceptional efficiency, achieving inactivation rates of 99.97% and 99.93% for *S. aureus* and *E. coli*, respectively, surpassing the performance of free curcumin. The superior performance of Lys-AuNCs-Cur is attributed to several nanoscale enhancements. It showed markedly improved aqueous solubility (333.6 μg/mL vs. 0.102 μg/mL for free curcumin), increased photostability (only 19% degradation after 24 h of sunlight vs. 74% for free curcumin), and enhanced ROS and $^1O_2$ production. Its positive surface charge (+42 mV) enabled strong electrostatic interaction with negatively charged bacterial membranes, thereby facilitating targeted delivery and improved membrane disruption. Furthermore, the system exhibited a fluorescence resonance energy transfer (FRET) effect between the gold nanoclusters and curcumin, increasing fluorescence intensity for bacterial imaging and confirming successful interaction at the microbial interface. Fluorescence microscopy and SEM visualized pronounced bacterial membrane damage, while nucleic acid leakage (Abs260) confirmed the loss of integrity of cellular structures. Importantly, Lys-AuNCs-Cur also exhibited high biocompatibility, with >90% viability in normal hepatocyte (L-02) cells at concentrations up to 400 μg/mL, indicating its safety for therapeutic applications [22].

Metal–organic frameworks (MOFs) and covalent organic frameworks (COFs) have also emerged as highly versatile nanocarriers in curcumin-based aPDT. These platforms offer structural tunability, high surface area, and exceptional drug loading capabilities. More importantly, they address major limitations of free curcumin, such as poor water solubility, rapid degradation, and non-specific targeting [55,60,61]. MOFs, such as ZIF-8-based systems, demonstrate excellent performance in delivering curcumin for antimicrobial applications. For example, Cur@ZIF-8 NPs achieved robust antibacterial effects against *E. coli* and *S. aureus* under blue light (420–430 nm, 2.2 mW/cm^2 for 1 h), primarily due to enhanced ROS generation and membrane disruption [57]. Moreover, hybrid composites like Cur/PCL@ZIF-8 films with ≥15% *w*/*w* curcumin reduced bacterial counts by 99.9%, showcasing the strong anti-adhesion and anti-biofilm capabilities of MOFs [56]. These systems not only protect curcumin from photodegradation but also enable sustained, light-triggered release and pH-responsive behavior, as evidenced by Cur-TTD@ZIF-8, which showed over 99.9% antibacterial activity along with imaging and anti-inflammatory functions [58].

COFs are also a promising new class of drug delivery systems for aPDT. Unlike MOFs, COFs are built from organic linkers connected through strong covalent bonds, giving them high thermal and chemical stability. Li et al. (2023) developed a COF-like NP by covalently integrating curcumin with tetrakis(4-carboxyphenyl)porphyrin (TCPP) to form TCPP-Cur NPs, which were then co-coordinated with copper (Cu) and sodium alginate (SA) to produce Cur-TCPP NPs COF hydrogels. This composite demonstrated a high curcumin loading capacity of 27.68% and pH-responsive drug release, with faster curcumin release under acidic conditions (pH 5.0–6.5), mimicking infected wound environments. Upon 660 nm light irradiation (0.4 W/cm^2 for 20 min), the hydrogel achieved near-complete bacterial eradication, 99.95% for *S. aureus* and 99.8% for *E. coli*, via synergistic photothermal and photocatalytic effects that increased membrane permeability and protein leakage. In a full-thickness rat wound model, the Cur-TCPP NPs COF hydrogel dressing significantly accelerated healing, enhanced collagen deposition and re-epithelialization, and promoted tissue regeneration by day 14. Immunostaining revealed reduced TNF-α and elevated IL-10 and VEGF expression, indicating strong anti-inflammatory and pro-angiogenic effects [61]. Cur -TCPP NPs COF hydrogels present a multifunctional, biocompatible strategy for infection-responsive wound healing. MOFs and COFs also contribute to improved photostability and selective targeting. Their frameworks protect curcumin from premature degradation while enabling stimuli-responsive behaviors, such as pH- or light-triggered drug release. Some MOFs like Cur@ZIF-8/PLL-CIP [55] further integrate targeting ligands and secondary antimicrobials (for example, ciprofloxacin), boosting efficacy against methicillin-resistant *S. aureus* (MRSA) and achieving 99.83% biofilm disruption. Likewise, Cur-Zn-MOF@Ti_3C_2Tx nanosheets combined NIR-responsive Zn^{2+}/curcumin release, ROS generation, and photothermal therapy to kill *S. aureus*/*E. coli* and accelerate infected wound healing (>99% closure in 8 days) [60]. The integration of MOFs and COFs into curcumin-based aPDT platforms represents a powerful strategy to overcome curcumin's physicochemical limitations, achieve deep-tissue therapeutic targeting, and enhance bactericidal activity through multi-modal mechanisms. Data from Table 3 clearly support their superior performance in eradicating pathogens, controlling inflammation, and promoting wound healing, marking a significant advancement in nanotherapeutics for infectious disease management.

3.2.2. Structural and Functional Characteristics of Curcumin Nanocarriers

While Table 3 highlights the antimicrobial efficacy and photodynamic outcomes of various curcumin-loaded nanocarriers, Table 4 builds on this by providing critical structural and functional insights into these same platforms. Specifically, it presents key physicochemical parameters, such as particle size, zeta potential, drug encapsulation efficiency (EE%), release kinetics, and biocompatibility, that collectively influence the therapeutic performance and safety of curcumin-based nanocarriers in aPDT applications.

Table 4. Structural and functional characteristics of curcumin-based nanocarriers for aPDT: particle size, zeta potential, drug loading, release kinetics, and toxicity.

NPs	Particle Size, Zeta Potential	Drug Loading Rate and Release Kinetics	Toxicity	Ref
Curcumin-loaded Chitosan (CT) NPs	122 ± 2 nm	Cur-CT NPs demonstrated a high curcumin encapsulation efficiency of 96%, indicating excellent drug loading capacity. They also exhibited a controlled and sustained release profile, with only 17% of curcumin released over 400 min, in contrast to 50% release from free curcumin within the same timeframe	-	[13]

Table 4. *Cont.*

NPs	Particle Size, Zeta Potential	Drug Loading Rate and Release Kinetics	Toxicity	Ref
Curcumin loaded chitosan/sodium alginate NPs (Cur-CT-Alg NPs)	257.2 to 473.1 nm, −33.0 to −26.5 mV	The NPs showed high curcumin encapsulation efficiency (64.13–80.23%), with the highest at a CT:Alg ratio of 0.30:1. Higher ratios reduced EE% to ~33%. In simulated saliva (pH 7), Cur-CT-Alg NPs exhibited sustained release, with ~50% of curcumin released over 24 h, demonstrating effective drug retention.	The Cur-CT-Alg NPs showed excellent biocompatibility, and their use in aPDT achieved a 3-$\log_{10}$ CFU/mL reduction in *S. mutans* biofilms without toxicity.	[52]
Curcumin-containing chitosan-shelled nanobubbles, (Cur-CT-NBs)	511 ± 25 nm +30 ± 2 mV.	Cur-CT-NBs and Cur-Oxy-CT-NBs demonstrated curcumin loading capacities of 4.3% and 5.3%, respectively, with high encapsulation efficiencies ranging from 80% to 88%. Curcumin was successfully incorporated into both the nanobubble core and the chitosan shell, with slightly higher EE and LC observed in Cur-Oxy-CT-NBs. In vitro release studies showed sustained release, with 69.14% and 66.98% of curcumin released from Cur-CT-NBs and Cur-Oxy-CT-NBs after 48 h, respectively.	Biocompatible oxygen- and curcumin-loaded NBs exhibited antimicrobial activity via ROS generation under LED irradiation, damaging bacterial membranes without harming human cells. Curcumin's antioxidant effect within NBs reduced oxidative stress markers, supporting safe, eco-friendly antimicrobial applications.	[39]
Oxygen-loaded curcumin-containing nanobubbles, (Cur-Oxy-CT-NBs)	521 ± 30 nm +31 ± 1 mV			
Curcumin-loaded solid lipid NPs (SLNPs-composed of cetyl palmitate and Tween® 80) within an alginate-based hydrogel matrix	-	Curcumin-loaded SLNs were added to hydrogels at 20% and 50%, containing 9.5 µg and 24 µg of curcumin per 0.5 mL. Both gels showed slow, steady release over 72 h at body pH, with no burst effect. About 40% of curcumin was released from the 20% gel and 70% from the 50% gel.	Cytocompatibility tests with human gingival fibroblasts (hGFs) showed high cell viability for all formulations, including those exposed to aPDT. After 24 h and even 3 days, metabolic activity remained comparable to controls. Immunostaining confirmed normal fibroblast morphology. Prior studies support the safety of curcumin-PDT below 500 mg/L for dental applications.	[14]
Indocyanine green (ICG) doped with nano-curcumin and conjugated with Metformin (Met) (Cur-ICG-Met NPs)	60–100 nm, −9.1 ± 1.3 mV	--	-	[53]

Table 4. *Cont.*

NPs	Particle Size, Zeta Potential	Drug Loading Rate and Release Kinetics	Toxicity	Ref
nCur-AgNPs-colistin (CL)	402.6 nm, nCur at 10.3 mV	-	An MTT assay confirmed the low cytotoxicity of nCur-AgNPs-colistin toward L929 fibroblasts, with cell viability ranging from 83.20% to 92.48% at FBIC concentrations for *P. aeruginosa* strains. Even at twice the FBIC, ~80% of cells remained viable.	[50]
Lysozyme (Lys)-gold nanocluster (AuNCs)-Cur conjugate, (Lys-AuNCs-Cur) (Lys-AuNCs)	5 nm +42 mV	-	Lys-AuNCs-Cur exhibited excellent biocompatibility, showing minimal cytotoxicity toward normal human hepatocyte (L-02) cells, with over 90% viability even at 400 µg/mL.	[22]
Cur-silica NPs	36 to 40 nm	Curcumin was loaded into silica NPs at a 10:1 SiO_2-to-curcumin ratio, achieving 5% loading. At 50 µg/mL of nanoformulation, the effective curcumin concentration is approximately 2.5 µg/mL—20 times lower than the equivalent free curcumin dose.	Cur-silica NPs had a less cytotoxic/phototoxic effect on HDF fibroblast cells	[51]
Curcumin encapsulated in poly (lactic-co-glycolic acid) (PLGA) NPs (Cur@PLGA-NPs)		The encapsulation efficiency (EE) of curcumin in Cur@PLGA NPs was 87.6 ± 3.25%, with a loading capacity (LC) of 8.42 ± 0.23%.	aPDT with 10% Cur@PLGA-NPs and blue laser was safe, showing no cell damage or plasma quality changes.	[54]
Curcumin encapsulated into zeolite imidazole framework-8 (ZIF-8) NPs, and coated with ethylated poly-L-lysine (PLL) and loaded with ciprofloxacin (CIP) (Cur@ZIF-8 NPs/PLL-CIP)	325.9 nm −4.57 mV at pH 7.4 and −6.19 mV at pH 5.5	The drug loading capacity was 16.2% for CIP and 3.3% for Cur. At physiological pH (7.4), the 48 h release rates were 41.6% for Cur and 43.3% for CIP. Upon the addition of 2 mM H_2O_2, these rates increased to 66.1% for Cur and 64.7% for CIP. Under acidic conditions (pH 5.5) in the presence of H_2O_2, release rates further increased to 77.4% for Cur and 70.9% for CIP.	In vitro tests showed 69.1% HUVEC viability at 100 µg/mL, and only 2.1% haemolysis at 700 µg/mL, indicating good biocompatibility. In vivo, treated mice showed no weight loss or organ toxicity. Histological analysis revealed no tissue damage, and renal and hepatic function markers (AST, ALT, UREA, CREA, ALB) remained within normal ranges, confirming excellent biosafety.	[55]

Table 4. *Cont.*

NPs	Particle Size, Zeta Potential	Drug Loading Rate and Release Kinetics	Toxicity	Ref
Curcumin/polycaprolactone@zeolitic imidazolate framework-8 (Cur/PCL@ZIF-8) composite film	~100–200 nm	35% *w*/*w* Cur@ZIF-8 was loaded in PCL. Cur in the Cur/PCL film was rapidly released within 6 h, significantly exceeding that from the Cur/PCL@ZIF-8 composite film. Absorbance at 424 nm increased with time and higher Cur@ZIF-8 content, indicating sustained release. After 72 h, curcumin release under acidic conditions was nearly twice that under neutral conditions, demonstrating the film's pH-responsive and controlled-release properties.	-	[56]
Cur@ZIF-8 NPs	150 nm (while ZIF-8 alone was 80 nm)	Cur@ZIF-8 NPs exhibited a drug loading capacity of 11.57% and an encapsulation efficiency of 82.76%. Cur@ZIF-8 NPs exhibited pH-sensitive release behavior, maintaining high Cur retention rates at neutral to alkaline pH—93.38% at pH 7.4, 96.19% at pH 9, and 93.01% at pH 10 over 72 h—indicating excellent stability of Cur within the ZIF-8 framework. In contrast, under acidic conditions (pH 5.5 and 6.5), a burst release was observed during the initial 8 h, with cumulative Cur release reaching approximately 60% and 70%, respectively, demonstrating effective pH-triggered release for targeted antimicrobial applications.	-	[57]
Curcumin and aggregation-induced emission luminogen (TTD), encapsulated into ZIF-8 (Cur-TTD@ZIF-8 NPs)	360.84 nm	Drug-loading capacity (DLC) was 5.12%, and drug-loading encapsulation (DLE) was 20.46%. The release of Cur from Cur-TTD@ZIF-8 NPs is pH-dependent, showing high retention at pH 7.5. At pH 5.5 and 6.5, a rapid burst release occurred within 1 h, reaching ~70% cumulative release due to the acid-sensitive disintegration of ZIF-8	In vitro, the NPs maintained high cell viability in L929 (mouse fibroblast) and HUVEC (human umbilical vein endothelial) cells up to 250 µg/mL, with mild toxicity at 500 µg/mL due to excess Cur and Zn^{2+}. Hemolysis assays showed no adverse effects on red blood cells. In vivo, treatment in rats (125 µg/mL for 7 days) showed no abnormalities in blood tests or organ histology, indicating good biocompatibility.	[58]

Table 4. *Cont.*

NPs	Particle Size, Zeta Potential	Drug Loading Rate and Release Kinetics	Toxicity	Ref
Curcumin-based bioactive zinc-based metal–organic frameworks (Zn-MOF) and $Ti_3C_2T_x$ MXene nanosheets (NSs) (Cur/Zn-MOF@$Ti_3C_2T_x$)	lattice spacing of 0.22 nm	Curcumin from Cur/Zn-MOF@$Ti_3C_2T_x$ under NIR irradiation showed rapid release in the first 2 h, reaching 10.09 µg/mL at 48 h, 2.1× higher than the non-irradiated group. Similarly, Zn^{2+} release peaked at 3.64 µg/mL. NIR irradiation significantly enhanced initial release rates of both curcumin and Zn^{2+} within 12 h	Cur/Zn-MOF@$Ti_3C_2T_x$ exhibits excellent in vitro and in vivo biocompatibility, with >85% cell viability, <4% hemolysis, and minimal in vivo toxicity, even at 200 µg/mL.	[60]
Curcumin linked to tetrakis (4-carboxyphenyl) porphyrin TCPP (Cur-TCPP NPs) and co-coordinated with copper (Cu) and sodium alginate (SA) to form a covalent organic framework-like (COF-like) structure.	800 nm long TCPP, Cur, and TCPP-Cur were negatively charged. However, CuTCPP-Cur was positively charged	-	The Cur-TCPP NPs COF hydrogel showed excellent cytocompatibility in vitro and no organ toxicity in vivo. Minimal copper ion release and negligible hemolysis further confirmed its good biocompatibility and biosafety.	[61]

i. Particle Size and Zeta Potential

NP size and surface charge are critical determinants of nanocarrier behavior in biological environments, directly influencing biofilm penetration, cellular uptake, circulation dynamics, and interaction with microbial membranes [63]. The nanocarriers presented in Table 4 exhibit a broad size distribution, from ultra-small gold nanoclusters (Lys-AuNCs-Cur, ~5 nm) to large, structured materials such as Cur-TCPP COF (~800 nm), demonstrating their design flexibility to address various therapeutic challenges in aPDT.

Smaller nanocarriers, typically under 150 nm, such as Cur-SiNPs (~40 nm) [51], Cur@ZIF-8 [57], and Cur-ICG-Met NPs [53], possess enhanced mobility through dense biological matrices. Their reduced size facilitates deeper diffusion into biofilms and infected tissues, leading to more efficient intracellular delivery and greater photodynamic damage upon light activation. These properties correspond with the potent antimicrobial effects observed in Table 3, especially in eradicating biofilm-associated pathogens and intracellular infections. On the other hand, larger carriers like Cur-TCPP COF (~800 nm long) [61] and Cur-Oxy-CT-NBs (521 ± 30 nm) [39], although restricted in tissue penetration due to their size are advantageous for localized treatments. Their extended surface residence allows prolonged photodynamic action on superficial infections or wounds [64], where deep penetration is not a therapeutic priority.

Surface charge, often measured as zeta potential, further modulates NP–cell interactions. Cationic systems such as Lys-AuNCs-Cur (+42 mV) [22] and Cur-CT-NBs (+30 mV) [39] exhibit strong electrostatic attraction to the negatively charged bacterial cell envelopes. This promotes rapid adhesion, enhances cellular internalization, and improves ROS-mediated bacterial destruction, key advantages for boosting the aPDT mechanism. The significance of these features is highlighted by the markedly higher bactericidal outcomes these systems achieved, as detailed in Table 3.

These findings show the importance of rational NP design. Tailoring particle size and zeta potential enables the optimization of curcumin delivery and activation, ultimately enhancing its antimicrobial efficacy while minimizing off-target effects.

ii. Drug Loading Capacity and Release Kinetics

Efficient encapsulation and controlled release of curcumin are critical for maintaining therapeutic drug levels, reducing degradation, and enhancing antimicrobial efficacy during aPDT [4,65]. As shown in Table 4, several nanocarrier systems demonstrate high drug loading capacities and favorable release profiles, key properties that directly support the enhanced aPDT. For example, high drug loading efficiencies were observed in systems such as Cur@PLGA (87.6%) [54], Cur-CT (96%) [13], and Cur@ZIF-8 (82.76%) [57]. These values reflect the effective incorporation of curcumin within the carrier matrix, ensuring an adequate payload for sustained therapeutic action. The high encapsulation efficiencies also contribute to improved photostability and retention of curcumin's bioactive properties during storage and delivery.

Several formulations exhibit prolonged and sustained drug release, which is essential for long-term antimicrobial action, particularly in chronic or biofilm-associated infections. Cur-CT-Alg [52], solid lipid NPs [14], Cur-TTD@ZIF-8 [58], and Cur-CT [13] all demonstrated slow-release kinetics that enhance curcumin bioavailability. For example, Cur-CT released only ~17% of curcumin over 400 min, while free curcumin released nearly 50% within the same period, [13] confirming the superior control over drug release provided by nanoformulation.

Furthermore, stimuli-responsive nanocarriers introduce an advanced level of control by enabling environment-specific drug release. For instance, Cur/PCL@ZIF-8 [56] and Cur/Zn-MOF@Ti_3C_2Tx [60] exhibited pH and light-triggered curcumin release, respectively, enabling targeted drug liberation in acidic microenvironments typical of infected tissues and biofilms. This targeted behavior enhances therapeutic specificity, reduces systemic side effects, and supports dual therapeutic functionalities such as bacterial killing and tissue regeneration. By integrating high drug-loading efficiency, sustained release, and stimuli-responsiveness, these nanocarriers effectively address the pharmacokinetic limitations of free curcumin, positioning them as promising candidates for safe and efficient aPDT-based antimicrobial therapies [66].

iii. Toxicity and Biocompatibility

The clinical translation of aPDT relies not only on potent antimicrobial activity but also on ensuring minimal toxicity to host tissues. Table 4 demonstrates that most curcumin-loaded nanocarriers maintain a favorable biosafety profile in both in vitro and in vivo models, reinforcing their suitability for clinical applications. In vitro cytocompatibility was consistently high across several formulations. For instance, Cur/Zn-MOF@$Ti_3C_2T_x$ [60], Lys-AuNCs-Cur [22], and nCur-AgNPs-colistin [50] all exhibited cell viability exceeding 85–90%. These results reflect minimal inherent cytotoxicity and support the safe use of these systems in wound healing or mucosal applications, where prolonged contact with host tissues is likely.

Phototoxicity assessments further confirmed the safety of these systems under light exposure. For example, Cur-silica NPs [51] and Cur@PLGA [54] demonstrated negligible damage to healthy fibroblasts or epithelial cells upon irradiation, an essential criterion for PS-loaded platforms intended for therapeutic light activation. Additionally, in vivo toxicity evaluations provided compelling evidence of systemic biosafety. In studies involving animal models, Cur@ZIF-8/PLL-CIP [55] and Cur-TTD@ZIF-8 NPs [58] showed no signs of organ damage, inflammation, or hematological abnormalities following treatment. Histological and biochemical analyses confirmed the absence of adverse effects, thereby supporting the biocompatibility and low systemic toxicity of these advanced nanoplatforms. These findings show the importance of balancing efficacy with safety in the design of nanocarriers for aPDT. The demonstrated low toxicity profiles not only facilitate repeated applications but also increase the feasibility of applying these formulations in clinical settings for the treatment of chronic, drug-resistant, or biofilm-associated infections.

The use of nanotechnology to load curcumin onto specialized NP carriers offers a highly effective strategy to overcome the physicochemical and biological limitations of free curcumin. These platforms enable improved solubility, stability, selective targeting, and enhanced ROS-mediated phototoxicity, making them particularly suited for combating persistent and resistant microbial infections, including those involving biofilms and MDR strains. The data in Tables 3 and 4, highlight the importance of smart nanocarrier design in unlocking curcumin's full potential in aPDT and support its use in advanced antimicrobial treatments.

4. Applications of nCur and Curcumin-Based Nanocarriers in aPDT

nCur and curcumin-loaded NPs in aPDT have shown strong antimicrobial effects. By generating ROS when exposed to light, they can effectively target and destroy microbes. Applications include clinical areas like wound healing and dental care, as well as non-clinical uses such as disinfecting medical devices, treating water, and preserving food as illustrated in Figure 4.

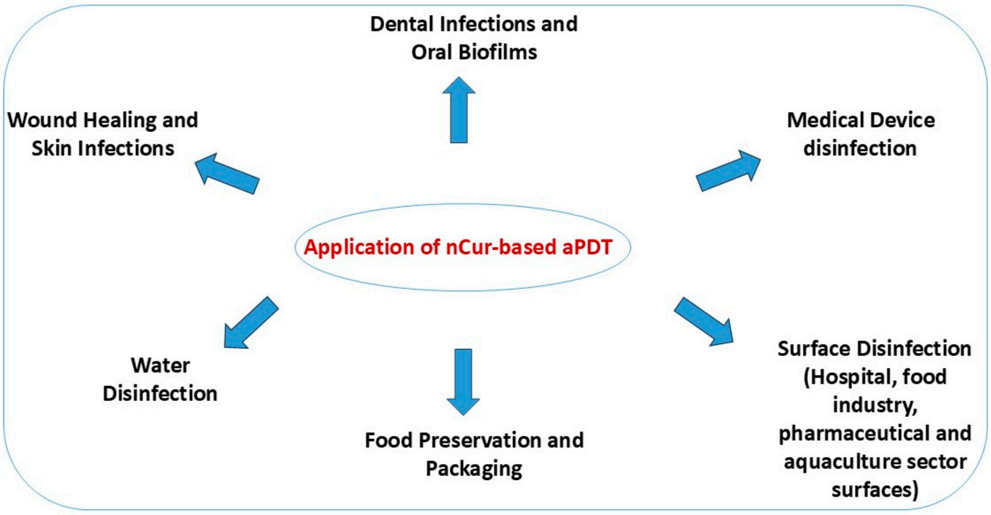

Figure 4. Illustration of the applications of nCur and curcumin-based nanocarriers in aPDT.

4.1. Wound Healing and Skin Infections

Topical application of nCur-based aPDT presents a highly promising and innovative approach for managing infected wounds, including burns and ulcers [51,67–69]. These wounds are often colonized by biofilm-forming, MDR pathogens such as *S. aureus*, *P. aeruginosa*, and *A. baumannii*, which impair healing and increase the risk of systemic infection [70]. Conventional topical antibiotics frequently fail in such cases due to limited tissue penetration and AMR, necessitating alternative strategies. nCur-based aPDT addresses these limitations using light-activated curcumin delivered in nanocarriers, which overcome curcumin's inherent issues of poor solubility, low bioavailability, and instability [71]. Polymers such as PLGA, chitosan, and poly (L-lactic acid) enable controlled release, enhanced photostability, and deep tissue penetration, features essential for effective infection control and tissue repair [13,54,72].

Studies have shown that curcumin-loaded silica NPs, activated by blue light (465 nm, 20 J/cm^2), achieve over 6 $\log_{10}$ CFU reduction in planktonic bacterial forms and more than

5 $\log_{10}$ in biofilms. These NPs also promoted fibroblast migration in scratch assays, indicating enhanced wound healing potential, and exhibited no significant toxicity at therapeutic doses [51]. In rodent models, various curcumin nanoformulations have demonstrated strong dual-action benefits. Ethosomal curcumin inhibited *P. aeruginosa* and improved second-degree burn healing; curcumin-chitosan-PEG NP reduced MRSA and *P. aeruginosa* viability while accelerating wound closure and neovascularization; PLGA-curcumin enhanced re-epithelialization and collagen synthesis; and hydrogels and pluronic gels further supported tissue regeneration, including in diabetic wounds [72].

Importantly, CurNisNP, a poly(L-lactic acid) NP formulation co-loaded with curcumin and the antimicrobial peptide nisin, demonstrated a 71.4% reduction in *A. baumannii* biofilm mass in a murine burn wound model. This formulation successfully combined the antimicrobial and anti-inflammatory effects of curcumin with the bactericidal activity of nisin, resulting in improved infection control and wound healing [73]. Safety assessments showed minimal host tissue damage, and evidence suggests that curcumin-based aPDT may also normalize epithelial markers such as cytokeratins CK13 and CK14, supporting tissue recovery [72].

Altogether, nanocurcumin-based aPDT offers a safe, non-antibiotic, and multifunctional strategy for treating infected wounds by effectively eliminating biofilms, reducing microbial burden, and accelerating tissue regeneration. Its versatility and efficacy make it a compelling candidate for clinical translation in the management of complex, drug-resistant skin infections across human, veterinary, and aquatic settings.

4.2. Dental Infections and Oral Biofilms

Nanocurcumin-based aPDT (nCur-aPDT) is an emerging, non-invasive approach for managing a wide range of dental and oral infections, particularly those involving treatment-resistant microbial biofilms [11,74,75]. It has shown efficacy against key pathogens such as *S. mutans*, *E. faecalis*, *L. acidophilus*, and *C. albicans*, which are implicated in dental caries, endodontic reinfections, periodontal disease, and oral candidiasis [11,14,76]. Nanocarriers, including polymeric NPs, micelles, and solid lipid NPs, enhance the delivery of curcumin by improving solubility, bioavailability, and penetration into biofilms, which upon activation with light, curcumin generates ROS that disrupt microbial cells and biofilm structure, reducing virulence while sparing host tissues [13,54].

Several studies support the clinical potential of nCur-aPDT. In periodontal and endodontic applications, curcumin-loaded SLNPs incorporated into an alginate-PVA hydrogel achieved up to 70% reduction in *E. faecalis* biofilms and maintained antibacterial activity for three days, while preserving fibroblast viability, highlighting its promise as an intracanal medicament [14]. Similarly, nano-micelle curcumin showed a 40% reduction in dual-species biofilms of *S. mutans* and *L. acidophilus* grown on enamel slabs, outperforming hydrogen peroxide and riboflavin-based PDT, with no adverse effect on enamel mineral content after 21 days [11].

In restorative dentistry, nCur incorporated into Activa BioActive Base/Liner (ABBL) significantly inhibited *S. mutans* biofilm growth. When activated by LED light (435 ± 20 nm), 5% nCur-ABBL disks achieved a 97.5% bacterial reduction after 60 days in artificial saliva, demonstrating long-term antimicrobial efficacy [43]. Additionally, a dual-modal composite of reduced graphene oxide–nCur (rGO-nCur), coated onto orthodontic elastomeric ligatures, demonstrated significant biofilm inhibition through combined photodynamic inactivation (450 nm) and photothermal inactivation (980 nm). This system achieved an 83.6% reduction in *S. mutans* biofilms, a 96.2% decrease in extracellular polysaccharide production, and notable downregulation of key virulence genes, all while preserving the mechanical integrity of the ligatures [74].

Clinical trials reinforce these findings. Although clinical data specifically on nCur are limited, existing trials using native curcumin support its efficacy in aPDT. In AIDS patients, full-mouth aPDT with 0.75 mg/mL curcumin and 450 nm blue LED light significantly reduced *Streptococcus* spp. ($p = 0.023$), *Staphylococcus* spp. ($p = 0.001$), and total microbial load ($p = 0.017$), regardless of TCD4+ status. Reduced efficacy in those with low TCD8+ counts indicated some dependency on immune status [77]. Another trial in orthodontic patients used 1 g/L curcumin with 0.1% SDS to enhance delivery. The PDT + SDS group showed significant microbial reductions (5.44 ± 0.94 to 3.83 ± 0.71 log CFU/mL), comparable to chlorhexidine, without adverse effects [78].

Together, these findings confirm the clinical potential of nCur-aPDT for managing oral biofilms and infections. Its broad-spectrum antimicrobial activity, low cytotoxicity, anti-inflammatory and regenerative effects, and minimal risk of resistance make it a promising alternative to conventional therapies. nCur-aPDT has shown efficacy in diverse applications, including reducing bacterial load in periodontal pockets, enhancing root canal disinfection, promoting oral mucositis healing, and treating fungal and viral infections [79]. By overcoming key limitations of traditional antimicrobials, particularly against biofilm-associated pathogens, nCur-aPDT presents a versatile, non-invasive approach to improving oral healthcare outcomes. Future efforts should prioritize optimizing curcumin formulations, conducting large-scale clinical trials, and standardizing treatment protocols to support clinical translation and broader therapeutic use.

4.3. Medical Device and Surface Disinfection

nCur can be incorporated into coatings for medical devices such as catheters, orthopedic implants, and surgical meshes, offering a novel strategy for localized surface disinfection. When exposed to light, nCur generate ROS) that effectively degrade microbial cells and inhibit biofilm formation on device surfaces. The method enables contactless, residue-free disinfection that can be repeatedly activated through light exposure, making it a sustainable and efficient solution for infection control in healthcare settings [4,80]. For example, PSs such as methylene blue and Rose Bengal have been applied to surfaces for aPDT using a spray coating method. This process involves combining a UV-crosslinkable polymer, N-methyl-4(4′-formyl-styryl) pyridinium methosulfate acetal poly (vinyl alcohol) (SbQ-PVA), with the PS. The resulting PS-polymer solution is spray-coated onto commercial fabrics and materials, then cured under UV light to create a stable, light-activated antimicrobial layer [81]. This approach enables the fabrication of self-disinfecting surfaces, offering a practical and scalable strategy for infection control in healthcare and public environments.

4.4. Water Disinfection

nCur-aPDT offers a sustainable and effective approach to water disinfection, particularly in situations where conventional chemical treatments pose environmental or health risks [82]. Upon activation with blue light (405–460 nm), nCur generates ROS that effectively inactivate a broad range of waterborne pathogens, including *E. coli*, *Salmonella* spp., viruses, and protozoa [83], without producing harmful disinfection by-products. Its application is versatile; nCur can be embedded in filtration membranes, coated on water container surfaces, or applied in colloidal systems to enable localized, light-triggered antimicrobial action [4]. This method is non-toxic, biodegradable, and does not induce microbial resistance, making it a safe and eco-friendly alternative to chlorine-based disinfectants.

Experimental evidence supports its efficacy: curcumin combined with blue light rapidly inactivated aquatic pathogens such as *Vibrio cholerae*, *V. harveyi*, and *V. campbellii*. Significant reductions in cell viability were observed at submicromolar concentrations, with over 90% inactivation of *V. cholerae* and *V. harveyi* within minutes. ROS disrupted bacterial membranes, and survival increased only when antioxidants were introduced, confirming ROS as the key mechanism [82]. Additionally, the nanoscale formulation enhances curcumin's solubility, stability, and light absorption, improving performance even under low-intensity or natural light [71]. This makes nCur-aPDT particularly suitable for decentralized and off-grid water treatment systems, especially in rural or resource-limited regions, supporting the development of next-generation, green disinfection technologies aimed at improving public health and water safety.

4.5. Food Packaging and Surface Disinfection

nCur-aPDT presents an innovative, eco-friendly approach to improving food safety and prolonging shelf life. When incorporated into biodegradable packaging materials such as starch, polylactic acid, or cellulose, nCur enables light-activated antimicrobial activity directly on food surfaces [84–86]. Upon exposure to light, it generates ROS that effectively inactivate key foodborne pathogens, including *L. monocytogenes*, *Salmonella* spp., and *E. coli*. This strategy reduces microbial contamination, decreases the need for synthetic preservatives, and supports sustainable food preservation. As a non-toxic, naturally derived compound, curcumin aligns with the principles of green packaging technologies [84]. For instance, turmeric, a natural spice rich in curcumin, can be used to synthesize carbon quantum dots (TurCDs) with enhanced photodynamic efficiency. Embedding these TurCDs into a chitosan matrix, a biopolymer with inherent antibacterial properties, produces active packaging films (TurCDs-CT). Upon irradiation with 405 nm light, the TurCDs generate ROS that deactivate pathogens such as *S. aureus* and *E. coli*. These composite films demonstrate improved mechanical strength, UV protection, barrier properties, and thermal stability. In pork preservation trials, TurCDs-CT films significantly delayed spoilage and maintained sensory quality for up to 10 days [87].

aPDT also shows strong potential for fresh produce disinfection. Combining curcumin (5 mg/L) with UV-A light (320–400 nm) inactivated over 5 log CFU/mL of *E. coli* and *Listeria innocua* in produce wash water within 10 min. ROS generated by photoexcited curcumin disrupted bacterial membranes and DNA. Efficacy was further enhanced at acidic pH (pH 3.0) and remained effective at low temperatures (4 °C), even under high organic loads [88]. This method reduces reliance on chlorine sanitizers, avoids toxic by-products, and prevents cross-contamination, offering a safe, eco-friendly alternative for enhancing food safety in wash processes. In another study, Cur-aPDT reduced S. aureus by up to 5 log CFU/mL in pineapple and mango juices. At a light dose of 2.592 J/cm^2, no viable cells remained. ROS disrupted bacterial membranes and caused leakage of intracellular contents. However, efficacy varied with juice type, being lower in turbid or antioxidant-rich juices like carrot due to light scattering and ROS quenching. Despite minor color changes, this method offers a safe, non-thermal alternative for juice sanitation [20]. This biodegradable, light-responsive system offers a safe, sustainable alternative to conventional food packaging and disinfection methods.

5. Conclusions and Future Perspectives

5.1. Challenges and Future Directions

Despite encouraging preclinical outcomes, the clinical translation of curcumin-loaded nanocarriers for aPDT faces multiple challenges. A primary limitation is the lack of standardization and clinical validation. Most current studies are confined to in vitro systems or small animal models, limiting their translatability. Therefore, establishing standardized protocols for evaluating NP safety, dosing, light exposure parameters, and therapeutic outcomes is essential. Another critical barrier is the limited diffusion of NPs into dense biofilms and their tendency to aggregate in biological environments, which reduces therapeutic efficacy. Strategies such as NP size optimization (preferably <100 nm), surface modification with PEG or zwitterions, and enzyme-responsive carriers can improve biofilm penetration and minimize aggregation. Furthermore, the development of smart delivery systems, such as those that respond to infection-specific stimuli (e.g., pH or oxidative stress triggers), offers a promising path toward site-specific drug release and enhanced efficacy.

Looking ahead, combination therapies that co-deliver curcumin with conventional antibiotics, immune modulators, or metabolic inhibitors could yield synergistic effects and delay the onset of microbial resistance. Additionally, incorporating photothermal functionalities or immune-enhancing components may boost the therapeutic depth and breadth of aPDT. Technological advances, such as the integration of artificial intelligence, could streamline NP design, predict treatment outcomes, and support personalized therapy. Finally, interdisciplinary collaboration among nanotechnologists, microbiologists, clinicians, and regulatory experts will be essential to overcome regulatory hurdles and bring curcumin-based aPDT systems closer to clinical reality. Continued innovation in formulation science, delivery technologies, and validation frameworks will be key to unlocking the full potential of nCur-based aPDT in treating resistant infections.

5.2. Conclusions

Curcumin-loaded nanocarriers have emerged as promising tools in advancing aPDT, offering a potent alternative to overcome the inherent limitations of free curcumin, including poor solubility, chemical instability, rapid degradation, and low bioavailability. These nanoplatforms enhance ROS generation, enable site-specific and light-activated delivery, and improve curcumin's antimicrobial activity against multidrug-resistant pathogens and biofilms. Their versatility makes them suitable for applications in wound care, dental therapy, water purification, and food packaging. The integration of various nanocarrier systems, such as polymeric NPs, MOFs, COFs, and lipid-based formulations, has expanded the functional landscape of aPDT, demonstrating significant therapeutic promise across multiple domains.

Author Contributions: E.D.: literature search and manuscript writing; G.E.O.: Reviewing the manuscript. All authors have read and agreed to the published version of the manuscript.

Funding: This research received no external funding.

Institutional Review Board Statement: Not applicable.

Informed Consent Statement: Not applicable.

Data Availability Statement: New data was not generated for this study.

Conflicts of Interest: The author declares no conflicts of interest.

References

1. Aslam, B.; Asghar, R.; Muzammil, S.; Shafique, M.; Siddique, A.B.; Khurshid, M.; Ijaz, M.; Rasool, M.H.; Chaudhry, T.H.; Aamir, A.; et al. AMR and Sustainable Development Goals: At a Crossroads. *Glob. Health* **2024**, *20*, 73. [CrossRef]
2. Ho, C.S.; Wong, C.T.H.; Aung, T.T.; Lakshminarayanan, R.; Mehta, J.S.; Rauz, S.; McNally, A.; Kintses, B.; Peacock, S.J.; de la Fuente-Nunez, C.; et al. Antimicrobial Resistance: A Concise Update. *Lancet Microbe* **2025**, *6*, 100947. [CrossRef] [PubMed]
3. Afrasiyab; Zhou, R.; Raziq, K.; Xue, T.; Sun, D. Photodynamic Antibacterial Therapy by Metal Complex Mediators: A New Promise for Eliminating Drug-Resistant Infectious Microorganisms. *Inorganica Chim. Acta* **2025**, *587*, 122818. [CrossRef]
4. Dube, E. Antimicrobial Photodynamic Therapy: Self-Disinfecting Surfaces for Controlling Microbial Infections. *Microorganisms* **2024**, *12*, 1573. [CrossRef]
5. Da Silva, L.B.B.; Castilho, I.G.; de Souza Silva, F.A.; Ghannoum, M.; Garcia, M.T.; do Carmo, P.H.F. Antimicrobial Photodynamic Therapy for Superficial, Skin, and Mucosal Fungal Infections: An Update. *Microorganisms* **2025**, *13*, 1406. [CrossRef] [PubMed]

6. Ali, H.M.; Karam, K.; Khan, T.; Wahab, S.; Ullah, S.; Sadiq, M. Reactive Oxygen Species Induced Oxidative Damage to DNA, Lipids, and Proteins of Antibiotic-Resistant Bacteria by Plant-Based Silver Nanoparticles. *3 Biotech* **2023**, *13*, 414. [CrossRef]
7. Liu, Y.; Qin, R.; Zaat, S.A.J.; Breukink, E.; Heger, M. Antibacterial Photodynamic Therapy: Overview of a Promising Approach to Fight Antibiotic-Resistant Bacterial Infections. *J. Clin. Transl. Res.* **2015**, *1*, 140–167. [CrossRef]
8. Zhang, J.; Zhang, R.; Jin, S.; Feng, X. Curcumin, a Plant Polyphenol with Multiple Physiological Functions of Improving Antioxidation, Anti-Inflammation, Immunomodulation and Its Application in Poultry Production. *J. Anim. Physiol. Anim. Nutr.* **2024**, *108*, 1890–1905. [CrossRef]
9. Xu, F.; Hu, J.; Sriboonvorakul, N.; Lin, S. Evaluation of Antimicrobial Photodynamic Activity of CuminUP60®- A Commercially-Available High-Soluble Curcumin. *LWT—Food Sci. Technol.* **2024**, *205*, 116490. [CrossRef]
10. Lopresti, A.L. The Problem of Curcumin and Its Bioavailability: Could Its Gastrointestinal Influence Contribute to Its Overall Health-Enhancing Effects? *Adv. Nutr.* **2018**, *9*, 41–50. [CrossRef]
11. Afrasiabi, S.; AL. Gburi, A.Q.K.; Ranjbar Omrani, L.; Chiniforush, N.; Moradi, Z. Evaluation of Riboflavin, Nanocurcumin, and Hydrogen Peroxide under Light Conditions: Reduction of Mature Dental Biofilms and Enamel Mineral Loss. *Photodiagnosis Photodyn. Ther.* **2024**, *50*, 104379. [CrossRef]
12. Hassan, H.E.; Zaazou, M.H.; Sadony, D.M.; Mohamed, T.A. Effect of Diode Laser Irradiation and Application of Nanoparticle Herbal Endodontic Irrigation Solutions on Candida Albicans and Enterococcus Faecalis Bacteria. *Egypt. J. Chem.* **2024**, *67*, 331–340. [CrossRef]
13. Aguilera, L.F.; Araujo, L.O.; Facchinatto, W.M.; Lima, R.G.; da Silva Pontes, M.; Pulcherio, J.H.V.; Caires, C.S.A.; de Oliveira, K.T.; de Oliveira, S.L.; Caires, A.R.L. Blue-Light Photoactivated Curcumin-Loaded Chitosan Nanoparticles Prepared by Nanoprecipitation and Ionic Gelation: A Promising Approach for Antimicrobial Photodynamic Inactivation. *ACS Appl. Bio Mater.* **2025**, *8*, 4055–4064. [CrossRef]
14. Ferreira, S.; Grenho, L.; Fernandes, M.H.; Lima, S.A.C. Photoactivated Curcumin-Loaded Lipid Nanoparticles in Hydrogel: A Cutting-Edge Intracanal Medicament for Advanced Endodontic Therapy. *Gels* **2025**, *11*, 308. [CrossRef]
15. Chen, Y.; Lu, Y.; Lee, R.J.; Xiang, G. Nano Encapsulated Curcumin: And Its Potential for Biomedical Applications. *Int. J. Nanomed.* **2020**, *15*, 3099–3120. [CrossRef]
16. Mohanty, H.; Yadav, R.P. Nanoform of Curcumin: Expansion in Therapeutic Applications. *Adv. Tradit. Med.* **2024**, *25*, 39–55. [CrossRef]
17. Dias, L.D.; Blanco, K.C.; Mfouo-Tynga, I.S.; Inada, N.M.; Bagnato, V.S. Curcumin as a Photosensitizer: From Molecular Structure to Recent Advances in Antimicrobial Photodynamic Therapy. *J. Photochem. Photobiol. C Photochem. Rev.* **2020**, *45*, 100384. [CrossRef]
18. Hussain, Y.; Alam, W.; Ullah, H.; Dacrema, M.; Daglia, M.; Khan, H.; Arciola, C.R. Antimicrobial Potential of Curcumin: Therapeutic Potential and Challenges to Clinical Applications. *Antibiotics* **2022**, *11*, 322. [CrossRef] [PubMed]
19. Dang, Y.; Yang, R.; Jia, T.; Liu, C.; Geng, S. Curcumin-Mediated Antimicrobial Photodynamic Therapy for Inactivating Mycobacterium Abscessus: A Promising Approach for Non-Tuberculous Mycobacterial Skin Infections. *Lasers Med. Sci.* **2025**, *40*, 9. [CrossRef]
20. Yuan, Y.; Liu, Q.; Huang, Y.; Qi, M.; Yan, H.; Li, W.; Zhuang, H. Antibacterial Efficacy and Mechanisms of Curcumin-Based Photodynamic Treatment against Staphylococcus Aureus and Its Application in Juices. *Molecules* **2022**, *27*, 7136. [CrossRef] [PubMed]
21. Ahrari, F.; Mazhari, F.; Ghazvini, K.; Fekrazad, R.; Menbari, S.; Nazifi, M. Antimicrobial Photodynamic Therapy against Lactobacillus Casei Using Curcumin, Nano-Curcumin, or Erythrosine and a Dental LED Curing Device. *Lasers Med. Sci.* **2023**, *38*, 260. [CrossRef]
22. Zhang, Y.; Yan, H.; Su, R.; Li, P.; Wen, F.; Lv, Y.; Cai, J.; Su, W. Photoactivated Multifunctional Nanoplatform Based on Lysozyme-Au Nanoclusters-Curcumin Conjugates with FRET Effect and Multiamplified Antimicrobial Activity. *J. Drug Deliv. Sci. Technol.* **2022**, *74*, 103548. [CrossRef]
23. Ensafi, F.; Fazlyab, M.; Chiniforush, N.; Akhavan, H. Comparative Effects of SWEEPS Technique and Antimicrobial Photodynamic Therapy by Using Curcumin and Nano-Curcumin on Enterococcus Faecalis Biofilm in Root Canal Treatment. *Photodiagnosis Photodyn. Ther.* **2022**, *40*, 103130. [CrossRef]
24. Comeau, P.; Leite, M.L.; Manso, A. Development of a New Curcumin-Loaded Dental Varnish for Antimicrobial Photodynamic Therapy Application. *J. Biomed. Mater. Res.—Part B Appl. Biomater.* **2025**, *113*, e35596. [CrossRef] [PubMed]
25. Rodrigues, G.W.L.; Del Bianco Vargas Gouveia, S.; Oliveira, L.C.; de Freitas, R.N.; Dourado, N.G.; Sacoman, C.A.; Ribeiro, A.P.F.; Chaves-Neto, A.H.; Sivieri-Araújo, G.; de Toledo Leonardo, R.; et al. Comparative Analysis of Antimicrobial Activity and Oxidative Damage Induced by Laser Ablation with Indocyanine Green versus APDT with Methylene Blue and Curcumin on *E. coli* Biofilm in Root Canals. *Odontology* **2025**. [CrossRef] [PubMed]
26. Zupin, L.; Fontana, F.; Clemente, L.; Borelli, V.; Ricci, G.; Ruscio, M.; Crovella, S. Optimization of Anti-SARS-CoV-2 Treatments Based on Curcumin, Used Alone or Employed as a Photosensitizer. *Viruses* **2022**, *14*, 2132. [CrossRef]

27. Praditya, D.; Kirchhoff, L.; Brüning, J.; Rachmawati, H. Anti-Infective Properties of the Golden Spice Curcumin. *Front. Microbiol.* **2019**, *10*, 912. [CrossRef] [PubMed]
28. Julia, G.; Mika, M.; Wr, O.; Siudem, P. Methods to Improve the Solubility of Curcumin from Turmeric. *Life* **2023**, *13*, 207. [CrossRef]
29. Sohn, S.; Priya, A.; Balasubramaniam, B.; Muthuramalingam, P.; Sivasankar, C.; Selvaraj, A.; Valliammai, A.; Jothi, R.; Pandian, S. Biomedical Applications and Bioavailability of Curcumin—An Updated Overview. *Pharmaceutics* **2021**, *13*, 2102. [CrossRef]
30. Tsaplev, Y.B.; Lapina, V.A.; Trofimov, A.V. Curcumin in Dimethyl Sulfoxide: Stability, Spectral, Luminescent and Acid-Base Properties. *Dye. Pigment.* **2020**, *177*, 108327. [CrossRef]
31. Damyeh, M.S.; Mereddy, R.; Netzel, M.E.; Sultanbawa, Y. An Insight into Curcumin-Based Photosensitization as a Promising and Green Food Preservation Technology. *Compr. Rev. Food Sci. Food Saf.* **2020**, *19*, 1727–1759. [CrossRef]
32. Zhongfa, L.; Chiu, M.; Wang, J.; Chen, W.; Yen, W.; Fan-Havard, P.; Yee, L.D.; Chan, K.K. Enhancement of Curcumin Oral Absorption and Pharmacokinetics of Curcuminoids and Curcumin Metabolites in Mice. *Cancer Chemother. Pharmacol.* **2012**, *69*, 679–689. [CrossRef]
33. Yan, S.; Liao, X.; Xiao, Q.; Huang, Q.; Huang, X. Photostabilities and Anti-Tumor Effects of Curcumin. *RSC Adv.* **2024**, *14*, 13694–13702. [CrossRef]
34. Zhu, J.; Sanidad, K.Z.; Sukamtoha, E.; Zhang, G. Potential Roles of Chemical Degradation in the Biological Activities of Curcumin. *Food Funct.* **2017**, *8*, 907–914. [CrossRef]
35. Wolnicka-glubisz, A.; Olchawa, M.; Duda, M.; Pabisz, P.; Wisniewska-becker, A. The Role of Singlet Oxygen in Photoreactivity and Phototoxicity of Curcumin. *Photochem. Photobiol.* **2023**, *99*, 57–67. [CrossRef]
36. Rodrigues, F.M.S.; Tavares, I.; Aroso, R.T.; Dias, L.D.; Domingos, C.V.; de Faria, C.M.G.; Piccirillo, G.; Maria, T.M.R.; Carrilho, R.M.B.; Bagnato, V.S.; et al. Photoantibacterial Poly (Vinyl) Chloride Films Applying and Photosensitizers. *Molecules* **2023**, *28*, 2209. [CrossRef]
37. Li, Z.; Shi, M.; Li, N.; Xu, R. Application of Functional Biocompatible Nanomaterials to Improve Curcumin Bioavailability. *Front. Chem.* **2020**, *8*, 589957. [CrossRef] [PubMed]
38. Gera, M.; Sharma, N.; Ghosh, M.; Huynh, D.L.; Lee, S.J.; Min, T.; Kwon, T.; Jeong, D.K. Nanoformulations of Curcumin: An Emerging Paradigm for Improved Remedial Application. *Oncotarget* **2017**, *8*, 66680–66698. [CrossRef] [PubMed]
39. Munir, Z.; Molinar, C.; Banche, G.; Argenziano, M.; Magnano, G.; Cavallo, L.; Mandras, N.; Cavalli, R.; Guiot, C. Encapsulation in Oxygen-Loaded Nanobubbles Enhances the Antimicrobial Effectiveness of Photoactivated Curcumin. *Int. J. Mol. Sci.* **2023**, *24*, 15595. [CrossRef] [PubMed]
40. Wahnou, H.; El Kebbaj, R.; Liagre, B.; Sol, V.; Limami, Y.; Duval, R.E. Curcumin-Based Nanoparticles: Advancements and Challenges in Tumor Therapy. *Pharmaceutics* **2025**, *17*, 114. [CrossRef]
41. Dube, E.; Okuthe, G.E. Biobased Organic Nanoparticles: A Promising Versatile Green Tool for Novel Antimicrobial Agents for Improved Safety. *Int. J. Food Sci.* **2025**, *2025*, 7955106. [CrossRef] [PubMed]
42. Ahrari, F.; Nazifi, M.; Mazhari, F.; Ghazvini, K.; Menbari, S.; Fekrazad, R.; Babaei, K.; Banihashemrad, A. Photoinactivation Effects of Curcumin, Nano-Curcumin, and Erythrosine on Planktonic and Biofilm Cultures of Streptococcus Mutans. *J. Lasers Med. Sci.* **2024**, *15*, e7. [CrossRef]
43. Pourhajibagher, M.; Ranjbar Omrani, L.; Noroozian, M.; Ghorbanzadeh, Z.; Bahador, A. In Vitro Antibacterial Activity and Durability of a Nano-Curcumin-Containing Pulp Capping Agent Combined with Antimicrobial Photodynamic Therapy. *Photodiagnosis Photodyn. Ther.* **2021**, *33*, 102150. [CrossRef] [PubMed]
44. Pourhajibagher, M.; Talaei, N.; Bahador., A. Evaluation of Antimicrobial Effects of Photo-Sonodynamic Antimicrobial Chemotherapy Based on Nano-Micelle Curcumin on Virulence Gene Expression Patterns in Acinetobacter Baumannii. *Infect. Disord. Drug Targets* **2022**, *22*, 44–51. [CrossRef] [PubMed]
45. Shrestha, S.; Wang, B.; Dutta, P. Nanoparticle Processing: Understanding and Controlling Aggregation. *Adv. Colloid Interface Sci.* **2020**, *279*, 102162. [CrossRef]
46. Olaimat, A.N.; Ababneh, A.M.; Al-Holy, M.; Al-Nabulsi, A.; Osaili, T.; Abughoush, M.; Ayyash, M.; Holley, R.A. A Review of Bacterial Biofilm Components and Formation, Detection Methods, and Their Prevention and Control on Food Contact Surfaces. *Microbiol. Res.* **2024**, *15*, 1973–1992. [CrossRef]
47. Guo, Y.; Mao, Z.; Ran, F.; Sun, J.; Zhang, J.; Chai, G.; Wang, J. Nanotechnology-Based Drug Delivery Systems to Control Bacterial-Biofilm-Associated Lung Infections. *Pharmaceutics* **2023**, *15*, 2582. [CrossRef]
48. Jacob, S.; Kather, F.S.; Morsy, M.A.; Boddu, S.H.S.; Attimarad, M.; Shah, J.; Shinu, P.; Nair, A.B. Advances in Nanocarrier Systems for Overcoming Formulation Challenges of Curcumin: Current Insights. *Nanomaterials* **2024**, *14*, 672. [CrossRef]
49. Zhou, Z.; Li, P.; Chen, R.; Cai, X.; Zhang, W.; Fan, P.; Su, J. A Review of Curcumin-Mediated Photodynamic Bactericidal Technology for Food Preservation: Limitations and Improvement Strategies. *Food Microbiol.* **2025**, *131*, 104802. [CrossRef]
50. Azimzadeh, M.; Greco, G.; Farmani, A.; Pourhajibagher, M.; Taherkhani, A.; Alikhani, M.Y.; Bahador, A. Synergistic Effects of Nano Curcumin Mediated Photodynamic Inactivation and Nano-Silver@colistin against Pseudomonas Aeruginosa Biofilms. *Photodiagnosis Photodyn. Ther.* **2024**, *45*, 103971. [CrossRef]

51. Mirzahosseinipour, M.; Khorsandi, K.; Hosseinzadeh, R.; Ghazaeian, M.; Shahidi, F.K. Antimicrobial Photodynamic and Wound Healing Activity of Curcumin Encapsulated in Silica Nanoparticles. *Photodiagnosis Photodyn. Ther.* **2020**, *29*, 101639. [CrossRef]
52. Silvestre, A.L.P.; dos Santos, A.M.; de Oliveira, A.B.; Ferrisse, T.M.; Brighenti, F.L.; Meneguin, A.B.; Chorilli, M. Evaluation of Photodynamic Therapy on Nanoparticles and Films Loaded-Nanoparticles Based on Chitosan/Alginate for Curcumin Delivery in Oral Biofilms. *Int. J. Biol. Macromol.* **2023**, *240*, 124489. [CrossRef]
53. Pourhajibagher, M.; Plotino, G.; Chiniforush, N.; Bahador, A. Dual Wavelength Irradiation Antimicrobial Photodynamic Therapy Using Indocyanine Green and Metformin Doped with Nano-Curcumin as an Efficient Adjunctive Endodontic Treatment Modality. *Photodiagnosis Photodyn. Ther.* **2020**, *29*, 101628. [CrossRef]
54. Pourhajibagher, M.; Azimi, M.; Haddadi-asl, V.; Ahmadi, H. Photodiagnosis and Robust Antimicrobial Photodynamic Therapy with Curcumin-Poly(Lactic-Co-Glycolic Acid) Nanoparticles against COVID-19: A Preliminary in Vitro Study in Vero Cell Line as a Model. *Photodiagnosis Photodyn. Ther.* **2021**, *34*, 102286. [CrossRef]
55. Xiang, Y.-l.; Tang, D.-y.; Yan, L.-l.; Deng, L.-l.; Wang, X.-h.; Liu, X.-y.; Zhou, Q.-h. Poly-L-Lysine Modified MOF Nanoparticles with PH/ROS Sensitive CIP Release and CUR Triggered Photodynamic Therapy against Drug-Resistant Bacterial Infection. *Int. J. Biol. Macromol.* **2024**, *266*, 131330. [CrossRef] [PubMed]
56. Cai, Y.; Guan, J.; Wang, W.; Wang, L.; Su, J.; Fang, L. PH and Light-Responsive Polycaprolactone/Curcumin@zif-8 Composite Films with Enhanced Antibacterial Activity. *J. Food Sci.* **2021**, *86*, 3550–3562. [CrossRef]
57. Meng, X.; Guan, J.; Lai, S.; Fang, L.; Su, J. PH-Responsive Curcumin-Based Nanoscale ZIF-8 Combining Chemophotodynamic Therapy for Excellent Antibacterial Activity. *RSC Adv.* **2022**, *12*, 10005–10013. [CrossRef] [PubMed]
58. Li, X.; Wang, W.; Gao, Q.; Lai, S.; Liu, Y.; Zhou, S.; Yan, Y.; Zhang, J.; Wang, H.; Wang, J.; et al. Intelligent Bacteria-Targeting ZIF-8 Composite for Fluorescence Imaging-Guided Photodynamic Therapy of Drug-Resistant Superbug Infections and Burn Wound Healing. *Exploration* **2024**, *4*, 20230113. [CrossRef] [PubMed]
59. Henriques, J.; Pina, J.; Braga, M.E.M.; Dias, A.M.A.; Coimbra, P.; de Sousa, H.C. Novel Oxygen- and Curcumin-Laden Ionic Liquid@Silica Nanocapsules for Enhanced Antimicrobial Photodynamic Therapy. *Pharmaceutics* **2023**, *15*, 1080. [CrossRef]
60. Guo, C.; Cheng, F.; Liang, G.; Zhang, S.; Duan, S.; Fu, Y.; Marchetti, F.; Zhang, Z.; Du, M. Multimodal Antibacterial Platform Constructed by the Schottky Junction of Curcumin-Based Bio Metal–Organic Frameworks and Ti3C2Tx MXene Nanosheets for Efficient Wound Healing. *Adv. NanoBiomed Res.* **2022**, *2*, 2200064. [CrossRef]
61. Li, P.; Li, B.; Wang, C.; Zhao, X.; Zheng, Y.; Wu, S.; Shen, J.; Zhang, Y.; Liu, X. In Situ Fabrication of Co-Coordinated TCPP-Cur Donor-Acceptor-Type Covalent Organic Framework-like Photocatalytic Hydrogel for Rapid Therapy of Bacteria-Infected Wounds. *Compos. Part B* **2023**, *252*, 110506. [CrossRef]
62. Elkhateeb, O.; Badawy, M.E.I.; Tohamy, H.G.; Abou-ahmed, H.; El-kammar, M.; Elkhenany, H. Curcumin-Infused Nanostructured Lipid Carriers: A Promising Strategy for Enhancing Skin Regeneration and Combating Microbial Infection. *BMC Vet. Res.* **2023**, *19*, 206. [CrossRef]
63. Augustine, R.; Hasan, A.; Primavera, R.; Joyce, R.; Thakor, A.S.; Kevadiya, B.D. Cellular Uptake and Retention of Nanoparticles: Insights on Particle Properties and Interaction with Cellular Components. *Mater. Today Commun.* **2020**, *25*, 101692. [CrossRef]
64. Dragicevic, N.; Predic-Atkinson, J.; Nikolic, B.; Pajovic, S.B.; Ivkovic, S.; Adzic, M. Nanocarriers in Topical Photodynamic Therapy. *Expert Opin. Drug Deliv.* **2024**, *21*, 279–307. [CrossRef] [PubMed]
65. Costa, S.M.; Fangueiro, R.; Ferreira, D.P. Drug Delivery Systems for Photodynamic Therapy: The Potentiality and Versatility of Electrospun Nanofibers. *Macromol. Biosci.* **2022**, *22*, 2100512. [CrossRef] [PubMed]
66. Abdel-Mageed, H.M.; AbuelEzz, N.Z.; Ali, A.A.; Abdelaziz, A.E.; Nada, D.; Abdelraouf, S.M.; Fouad, S.A.; Bishr, A.; Radwan, R.A. Newly Designed Curcumin-Loaded Hybrid Nanoparticles: A Multifunctional Strategy for Combating Oxidative Stress, Inflammation, and Infections to Accelerate Wound Healing and Tissue Regeneration. *BMC Biotechnol.* **2025**, *25*, 49. [CrossRef]
67. Paolillo, F.R.; Gracielli, P.; Rodrigues, S.; Bagnato, V.S.; Alves, F.; Pires, L.; Corazza, A.V. The Effect of Combined Curcumin-Mediated Photodynamic Therapy and Artificial Skin on Staphylococcus Aureus—Infected Wounds in Rats. *Lasers Med. Sci.* **2021**, *36*, 1219–1226. [CrossRef]
68. Jansirani, D.; Muthulakshmi, L.; Gopukumar, S.T.; Rajeswari, R. Diabetic Wound Healing Effects of Photodynamic Therapy Using Chitosan Nanoparticles Encapsulated with Natural Photosensitizers in Wistar Rats. *Bionanoscience* **2025**, *15*, 376. [CrossRef]
69. Shanmugapriya, K.; Kang, H.W. Engineering Pharmaceutical Nanocarriers for Photodynamic Therapy on Wound Healing: Review. *Mater. Sci. Eng. C* **2019**, *105*, 110110. [CrossRef] [PubMed]
70. Ding, X.; Tang, Q.; Xu, Z.; Xu, Y.; Zhang, H.; Zheng, D.; Wang, S.; Tan, Q.; Maitz, J.; Maitz, P.K.; et al. Challenges and Innovations in Treating Chronic and Acute Wound Infections: From Basic Science to Clinical Practice. *Burn. Trauma* **2022**, *10*, tkac014. [CrossRef] [PubMed]
71. Karthikeyan, A.; Senthil, N.; Min, T. Nanocurcumin: A Promising Candidate for Therapeutic Applications. *Front. Pharmacol.* **2020**, *11*, 487. [CrossRef] [PubMed]

72. Sakima, V.T.; Barbugli, P.A.; Cerri, P.S.; Chorilli, M.; Carmello, J.C.; Pavarina, A.C.; De Oliveira Mima, E.G. Antimicrobial Photodynamic Therapy Mediated by Curcumin-Loaded Polymeric Nanoparticles in a Murine Model of Oral Candidiasis. *Molecules* **2018**, *23*, 2075. [CrossRef]
73. Pourhajibagher, M.; Pourakbari, B.; Bahador, A. Contribution of Antimicrobial Photo-Sonodynamic Therapy in Wound Healing: An in Vivo Effect of Curcumin-Nisin-Based Poly (L-Lactic Acid) Nanoparticle on Acinetobacter Baumannii Biofilms. *BMC Microbiol.* **2022**, *22*, 28. [CrossRef]
74. Ghanemi, M.; Salehi-Vaziri, A.; Pourhajibagher, M.; Bahador, A. Physico-Mechanical and Antimicrobial Properties of an Elastomeric Ligature Coated with Reduced Nanographene Oxide-Nano Curcumin Subjected to Dual-Modal Photodynamic and Photothermal Inactivation against Streptococcus Mutans Biofilms. *Photodiagnosis Photodyn. Ther.* **2023**, *44*, 103866. [CrossRef]
75. Bessa, L.J.; Botelho, J.; Machado, V.; Alves, R.; Mendes, J.J. Managing Oral Health in the Context of Antimicrobial Resistance. *Int. J. Environ. Res. Public Health* **2022**, *19*, 16448. [CrossRef]
76. Pourhajibagher, M.; Salehi Vaziri, A.; Takzaree, N.; Ghorbanzadeh, R. Physico-Mechanical and Antimicrobial Properties of an Orthodontic Adhesive Containing Cationic Curcumin Doped Zinc Oxide Nanoparticles Subjected to Photodynamic Therapy. *Photodiagnosis Photodyn. Ther.* **2019**, *25*, 239–246. [CrossRef]
77. Da Silva, F.C.; Rosa, L.P.; De Oliveira Santos, G.P.; Inada, N.M.; Blanco, K.C.; Araújo, T.S.D.; Bagnato, V.S. Total Mouth Photodynamic Therapy Mediated by Blue Led and Curcumin in Individuals with AIDS. *Expert Rev. Anti. Infect. Ther.* **2020**, *18*, 689–696. [CrossRef]
78. Panhóca, V.H.; Florez, F.L.E.; Corrêa, T.Q.; Paolillo, F.R.; de Souza, C.W.O.; Bagnato, V.S. Oral Decontamination of Orthodontic Patients Using Photodynamic Therapy Mediated by Blue-Light Irradiation and Curcumin Associated with Sodium Dodecyl Sulfate. *Photomed. Laser Surg.* **2016**, *34*, 411–417. [CrossRef] [PubMed]
79. Zhang, J.; Peng, Y.; Hu, S.; Xu, J.; Yu, C.; Hua, L.; Zhou, S.; Liu, Q. Therapeutic Application of Curcumin and Its Nanoformulation in Dentistry: Opportunities and Challenges. *AIMS Mol. Sci.* **2025**, *12*, 148–172. [CrossRef]
80. Gnanasekar, S.; Kasi, G.; He, X.; Zhang, K.; Xu, L.; Kang, E.T. Recent Advances in Engineered Polymeric Materials for Efficient Photodynamic Inactivation of Bacterial Pathogens. *Bioact. Mater.* **2023**, *21*, 157–174. [CrossRef] [PubMed]
81. Ghareeb, C.R.; Peddinti, B.S.T.; Kisthardt, S.C.; Scholle, F.; Spontak, R.J.; Ghiladi, R.A. Toward Universal Photodynamic Coatings for Infection Control. *Front. Med.* **2021**, *8*, 657837. [CrossRef]
82. Moideen, S.K.; Anas, A.; Sobhanan, J.; Zhao, H.; Biju, V. Photoeradication of Aquatic Pathogens by Curcumin for Clean and Safe Drinking Water. *J. Photochem. Photobiol. A Chem.* **2022**, *432*, 114104. [CrossRef]
83. Bhavya, M.L.; Umesh Hebbar, H. Efficacy of Blue LED in Microbial Inactivation: Effect of Photosensitization and Process Parameters. *Int. J. Food Microbiol.* **2019**, *290*, 296–304. [CrossRef]
84. Zhang, C.; Zhang, J.; Cao, S.; Tang, Y.; Wang, M.; Qu, C. Photodynamic Bactericidal Nanomaterials in Food Packaging: From Principle to Application. *J. Food Sci.* **2025**, *90*, e17606. [CrossRef] [PubMed]
85. Jacob, J.; Linson, N.; Mavelil-Sam, R.; Maria, H.J.; Pothan, L.A.; Thomas, S.; Kabdrakhmanova, S.; Laroze, D. *Poly(Lactic Acid)/Nanocellulose Biocomposites for Sustainable Food Packaging*; Springer: Dordrecht, The Netherlands, 2024; Volume 31, ISBN 0123456789.
86. Sheng, L.; Li, X.; Wang, L. Photodynamic Inactivation in Food Systems: A Review of Its Application, Mechanisms, and Future Perspective. *Trends Food Sci. Technol.* **2022**, *124*, 167–181. [CrossRef]
87. Wen, F.; Li, P.; Yan, H.; Su, W. Turmeric Carbon Quantum Dots Enhanced Chitosan Nanocomposite Films Based on Photodynamic Inactivation Technology for Antibacterial Food Packaging. *Carbohydr. Polym.* **2023**, *311*, 120784. [CrossRef] [PubMed]
88. de Oliveira, E.F.; Tosati, J.V.; Tikekar, R.V.; Monteiro, A.R.; Nitin, N. Antimicrobial Activity of Curcumin in Combination with Light against Escherichia Coli O157:H7 and Listeria Innocua: Applications for Fresh Produce Sanitation. *Postharvest Biol. Technol.* **2018**, *137*, 86–94. [CrossRef]